Statistical analysis in the search for dark photons from Higgs boson decays via ZH production with the ATLAS detector

MSc Thesis of Matthias Vigl

Supervisors: Prof. Marcello Fanti, Dr. Silvia Resconi, Dr. Federica Piazza

IMPRS Recruiting workshop, November 7 2022

ATLAS EXPERIMENT

Collaboration Site | Physics Results

ABOUT DISCOVER RESOURCES UPDATES SEARCH

All News Briefings Features Portraits Press Blog

Briefings

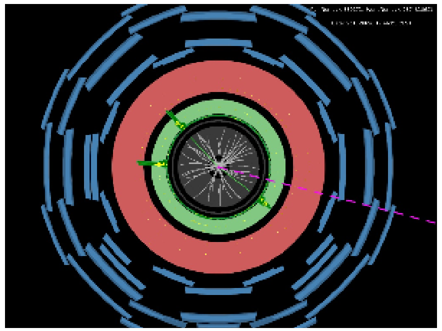

Using the Higgs boson to search for dark photons

The ATLAS Collaboration has been looking for signs of dark photons in data collected by the experiment during LHC Run 2 (2015-2018). Their newest search targets, for the first time in ATLAS, the production of a Higgs boson in association with a Z boson, with subsequent decay of the Higgs into a photon and a dark photon.

Physics Briefing | 15 September 2022

- Search for dark photon in $ZH, H \to \gamma\gamma_d$ channel: new analysis in ATLAS, using full Run 2
- My contributions: fit model (validation and final results), treatment of systematics and irreducible backgorund in the fit, optimization of binning in the Signal Region

Motivations:

- Dark Matter can be part of a Dark Sector, potentially interacting with the Standard Model Sector through portal interactions
- Dark-photon (γ_d) predicted as gauge boson of a new unbroken $U(1)_d$ group of the hypothetical Dark Sector
- The dark-photon can interact with SM sector through higher-dimensional interactions via messenger exchange: Loop of messenger fields can modify Higgs decay $H \to \gamma\gamma$

$$\implies \text{Higgs portal: } H \to \gamma\gamma_d$$

The Dark-Photon analysis at ATLAS

The Dark-Photon analysis:

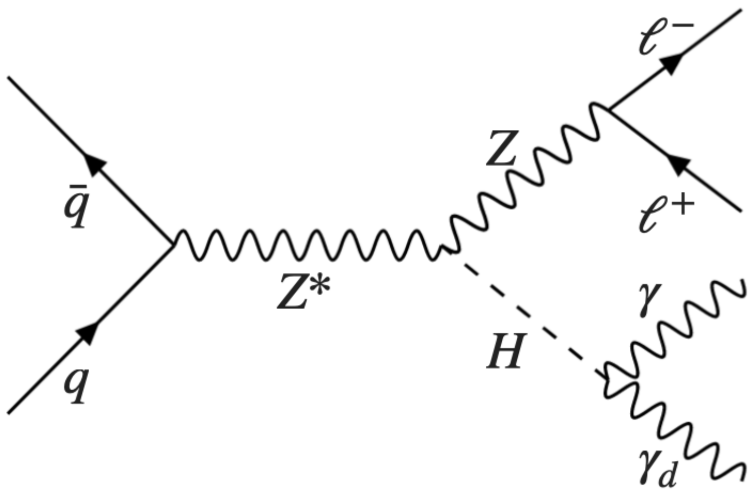

- Dark-photon from Higgs boson decay, in ZH production mode
- particles produced in pp collision at LHC
- γ_d invisible to the detector
  - total transverse momentum must balance
  - search for large transverse momentum imbalance: E_T^{miss}
- look for $\ell^+\ell^- + \gamma + E_T^{miss}$ events ($\ell = e, \mu$)
  - *ee channel* and *$\mu\mu$ channel*
  - eventually combined in the fit to data

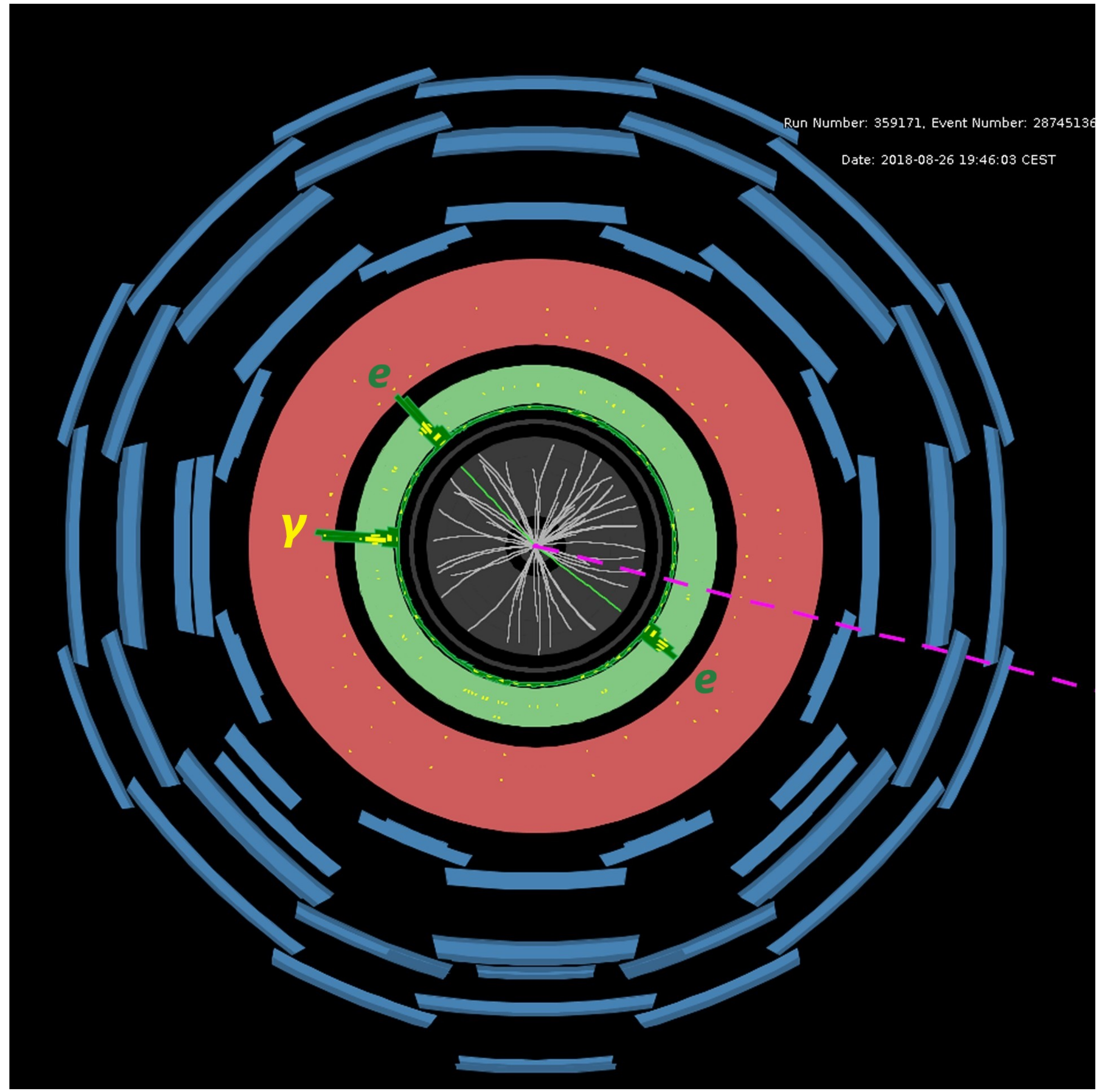

$$\vec{E}_T^{miss} = -\sum \vec{p}_T^{\,\mu} - \sum \vec{p}_T^{\,e} - \sum \vec{p}_T^{\,\gamma} - \sum \vec{p}_T^{\,\tau} - \sum \vec{p}_T^{\,jet} - \sum \vec{p}_T^{\,soft}$$

The Dark-Photon analysis:

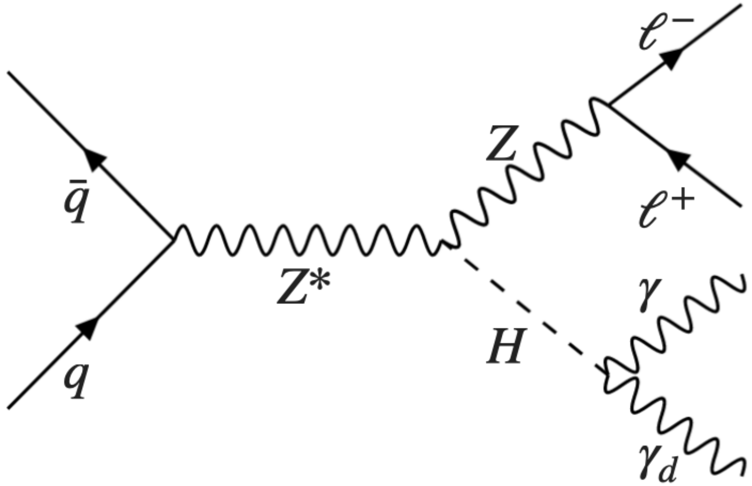

- Dark-photon from Higgs boson decay, in ZH production mode
- particles produced in *pp* collision at LHC
- γ_d invisible to the detector
  - total transverse momentum must balance
  - search for large transverse momentum imbalance: E_T^{miss}
- look for $\ell^+\ell^- + \gamma + E_T^{miss}$ events ($\ell = e, \mu$)
  - *ee channel* and $\mu\mu$ *channel*
  - eventually combined in the fit to data

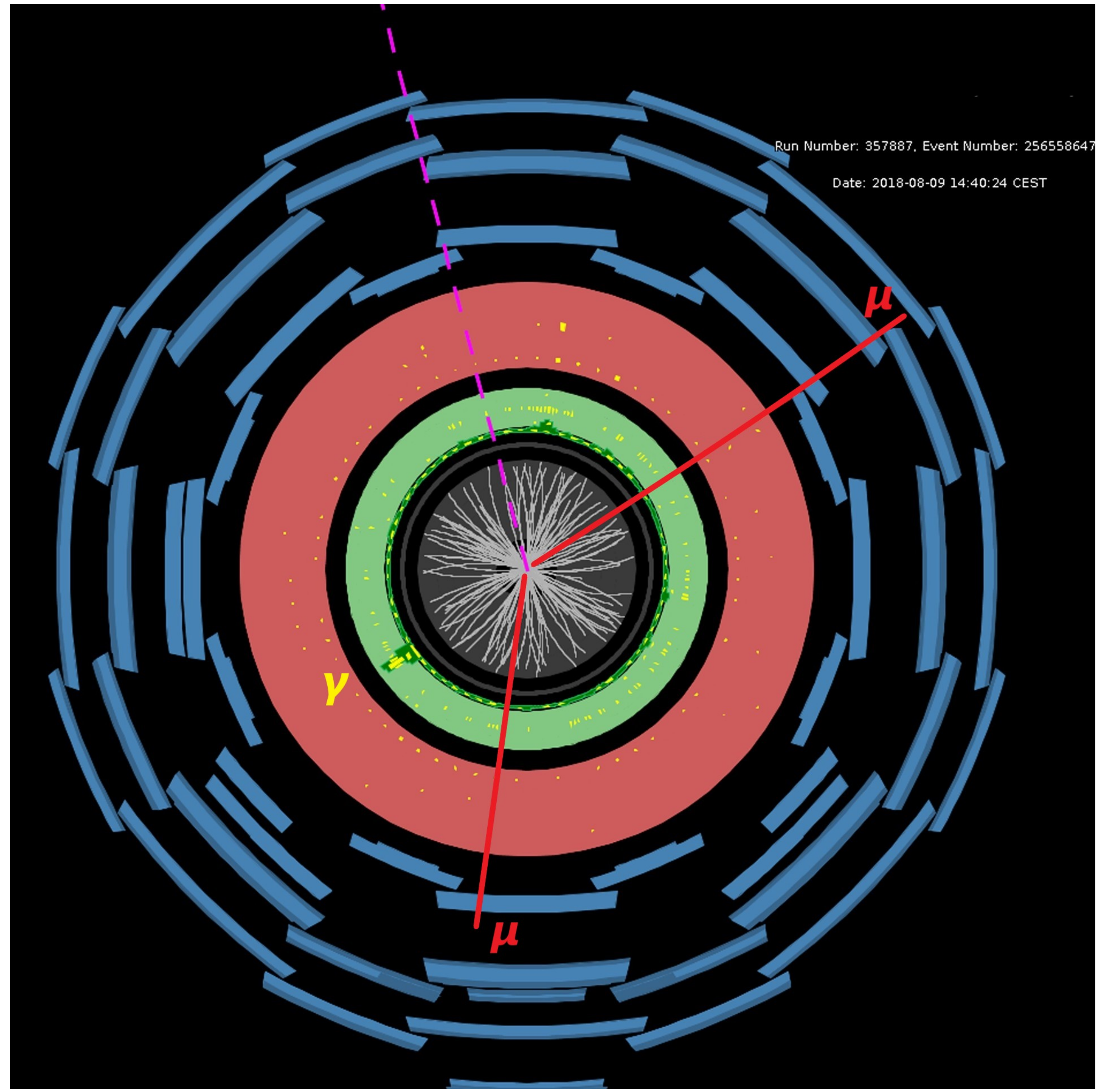

$$\vec{E}_T^{miss} = -\sum \vec{p}_T^{\,\mu} - \sum \vec{p}_T^{\,e} - \sum \vec{p}_T^{\,\gamma} - \sum \vec{p}_T^{\,\tau} - \sum \vec{p}_T^{\,jet} - \sum \vec{p}_T^{\,soft}$$

The Dark-Photon analysis at ATLAS

The Dark-Photon analysis:

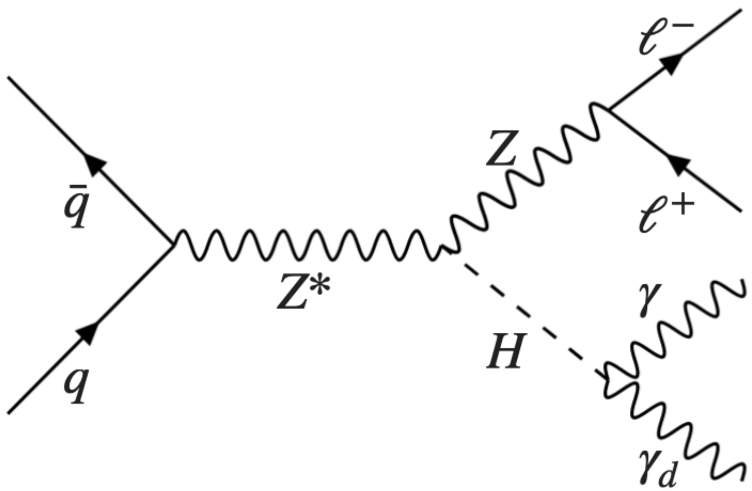

Signal Region (SR):

- 76 GeV $< m_{\ell\ell} <$ 116 GeV
- leading $\vec{p}_T^{\ell} >$ 27 GeV, sub-leading $\vec{p}_T^{\ell} >$ 20 GeV
- $\vec{p}_T^{\gamma} >$ 20 GeV
- Veto b-jet
- $\Delta\phi(\vec{E}_T^{miss}, \vec{p}_T^{\ell\ell\gamma}) >$ 2.4 rad

$E_T^{miss} >$ 60 GeV

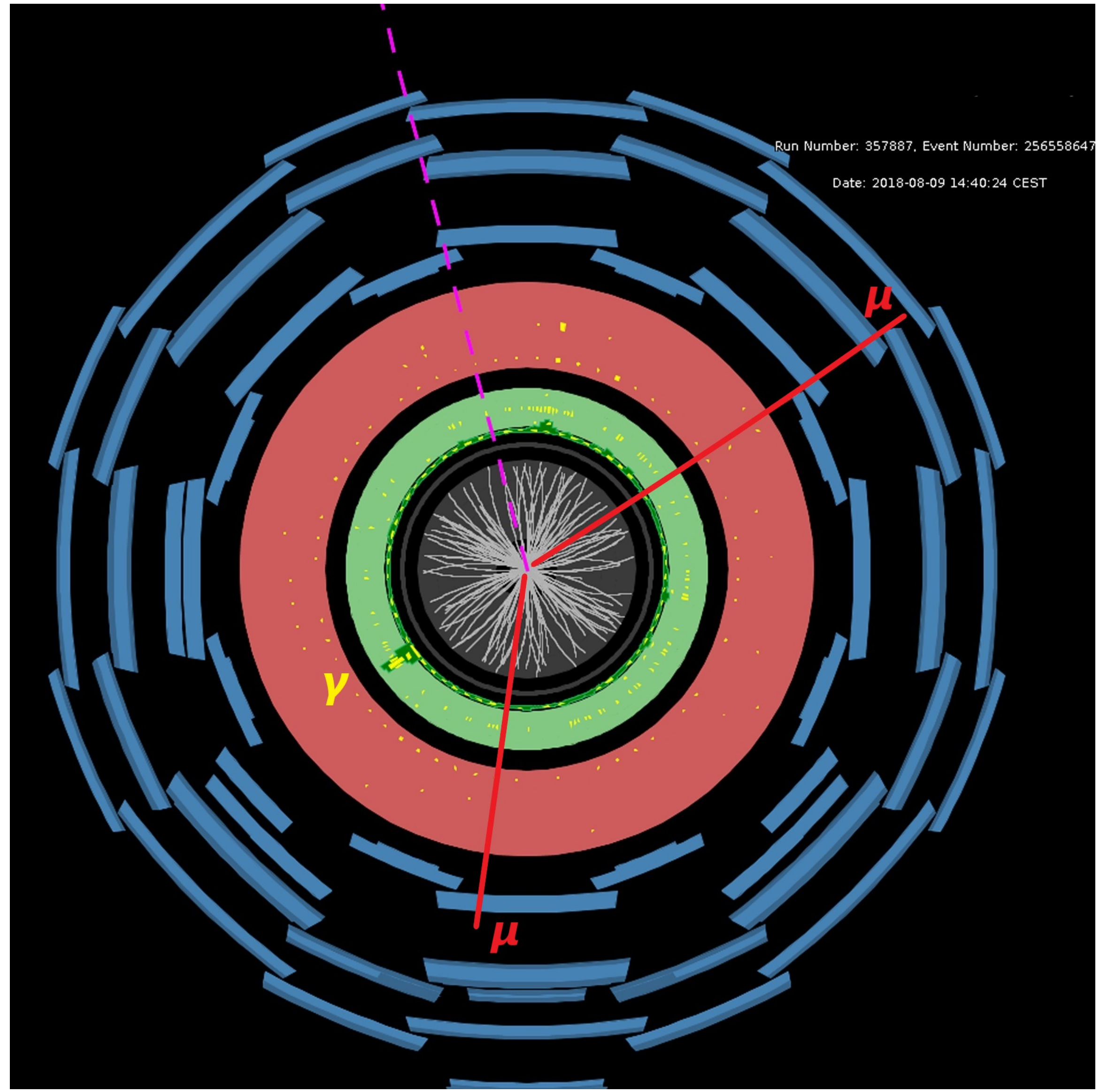

$$\vec{E}_T^{miss} = -\sum \vec{p}_T^{\mu} - \sum \vec{p}_T^{e} - \sum \vec{p}_T^{\gamma} - \sum \vec{p}_T^{\tau} - \sum \vec{p}_T^{jet} - \sum \vec{p}_T^{soft}$$

Backgrounds of the analysis

Background estimation: 6 background categories

- **Fake E_T^{miss}**: from $Z(\to \ell^+\ell^-)\gamma + jets$ and $Z(\to \ell^+\ell^-) + jets$
- **Fake photons from electrons e $\to \gamma$**: from $Z(\to \ell^+\ell^-)W(\to \ell\nu)$

due to jets mismeasurements or particle misidentification, Monte Carlo (MC) simulation not accurate enough
$\Longrightarrow$ use **data-driven estimates** with data control regions

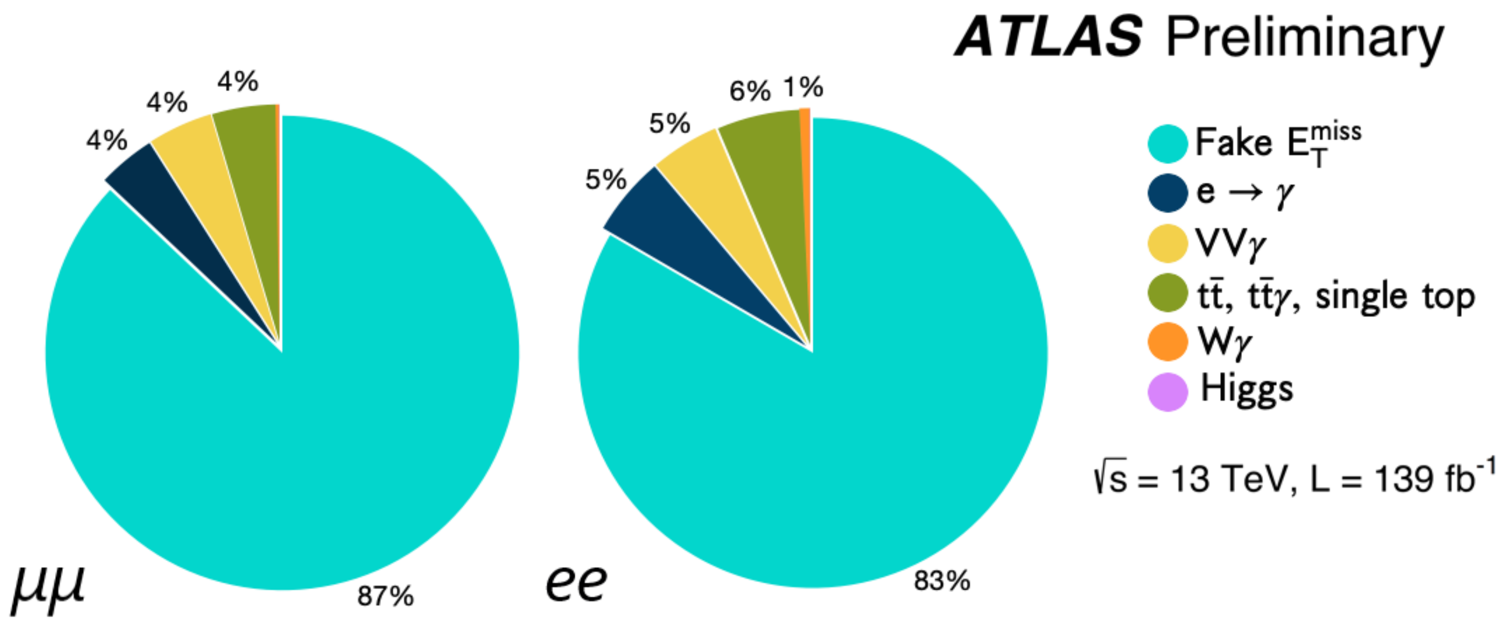

Backgrounds of the analysis

Background estimation: 6 background categories

- **Fake E_T^{miss}**: from $Z(\to \ell^+\ell^-)\gamma + jets$ and $Z(\to \ell^+\ell^-) + jets$
- **Fake photons from electrons e $\to \gamma$**: from $Z(\to \ell^+\ell^-)W(\to \ell\nu)$

due to jets mismeasurements or particle misidentification, Monte Carlo (MC) simulation not accurate enough
$\Longrightarrow$ use **data-driven estimates** with data control regions

- **VVy**: V(W,Z) bosons decaying leptonically $\Longrightarrow$ MC predictions corrected with a normalization factor ($k_{VV\gamma}$) obtained from data/MC comparison in a dedicated **Control Region (CR)** enriched of WZ process.

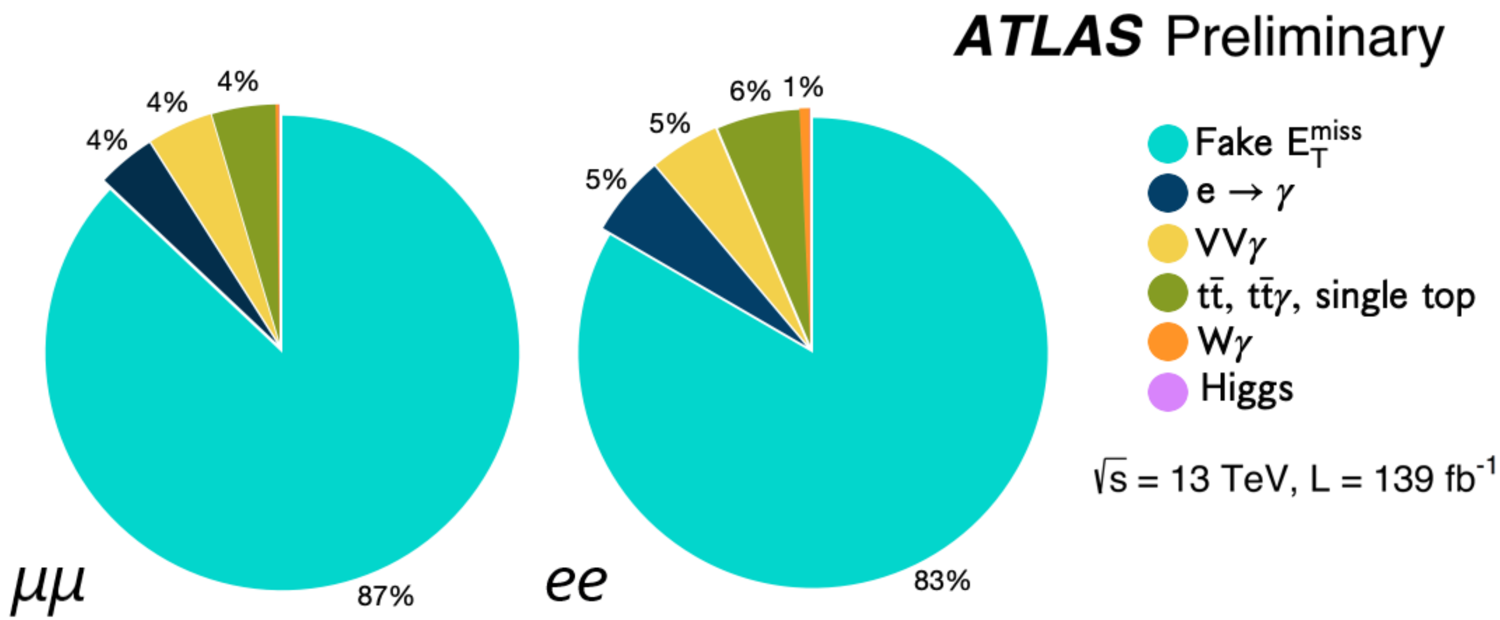

Backgrounds of the analysis

Background estimation: 6 background categories

- **Fake E_T^{miss}**: from $Z(\rightarrow \ell^+\ell^-)\gamma + jets$ and $Z(\rightarrow \ell^+\ell^-) + jets$
- **Fake photons from electrons e $\rightarrow \gamma$**: from $Z(\rightarrow \ell^+\ell^-)W(\rightarrow \ell\nu)$

due to jets mismeasurements or particle misidentification, Monte Carlo (MC) simulation not accurate enough
$\Longrightarrow$ use **data-driven estimates** with data control regions

- **VVy**: V(W,Z) bosons decaying leptonically $\Longrightarrow$ MC predictions corrected with a normalization factor ($k_{VV\gamma}$) obtained from data/MC comparison in a dedicated **Control Region (CR)** enriched of WZ process.
- **Top**: top quark production, with subsequest semi-leptonic $t \rightarrow W(\rightarrow \ell\nu)b$ decay $\Longrightarrow$ pure MC
- **Wy**, $\mathbf{H \rightarrow Z\gamma}$ $\Longrightarrow$ pure MC

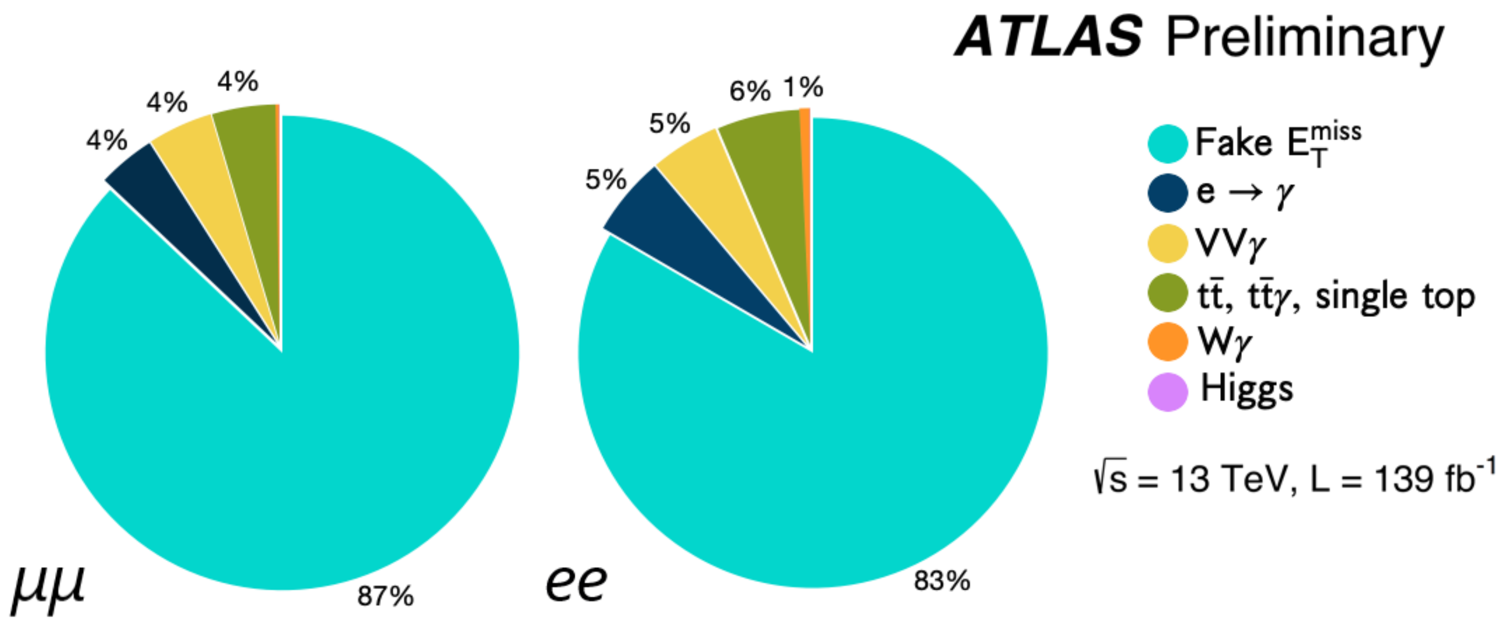

BDT discriminant variable

In order to increase the sensitivity of the analysis a Boosted Decision Tree (**BDT**) has been implemented:

- Trained on MC samples of background + signal, with most discriminant variables as input: E_T^{miss} significance, $m_T(\gamma, E_T^{miss})$, $m_{\ell\ell}$, $m_{\ell\ell\gamma}$, p_T^{γ}, $\frac{|\vec{E}_T^{miss}+\vec{p}_T^{\gamma}|-p_T^{\ell\ell}}{p_T^{\ell\ell}}$ in order of importance
- The BDT score is used as discriminant variable

- **Fake E_T^{miss}**, **e** $\rightarrow \gamma$, **VVy**, **Top**, **H** $\rightarrow$ **Z**γ, **Wy**

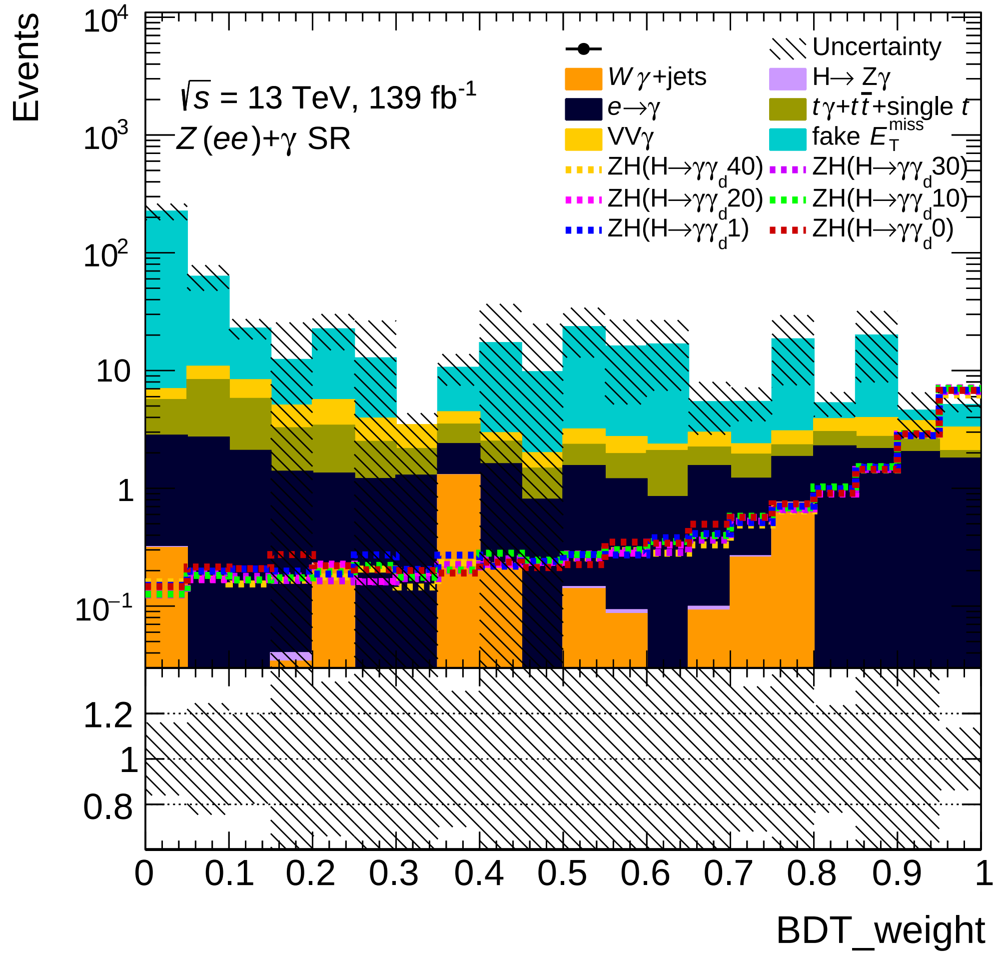

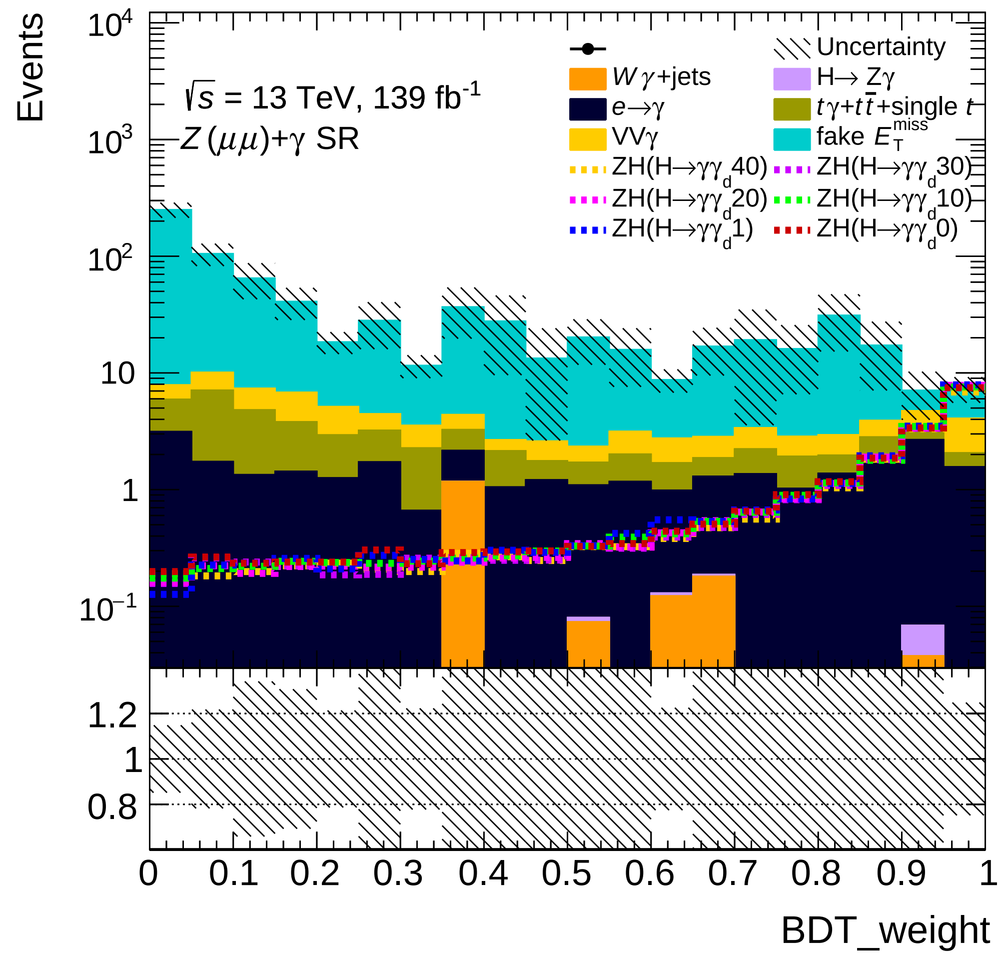

Fit strategy and statistical model

Binned maximum likelihood fit on BDT score distributions with $BR(H \to \gamma\gamma_d)$ as **parameter of interest**

6 background templates (one for each background category) + signal

Uncertainties included in the fit as **nuisance parameters (NP)** $\boldsymbol{\theta}$:

$$\mathcal{L}(data|\boldsymbol{k},\boldsymbol{\theta}) = \prod_{i \in BDT_{bins}+CR_{VV\gamma}} Pois(N_i^{data}|N_i^{exp}(\boldsymbol{k},\boldsymbol{\theta})) \times \prod_{j \in syst} G(\theta_j|0,1)$$

- $\boldsymbol{k} = [BR_{H\to\gamma\gamma_d}, k_{VV\gamma}]$
- $N_i^{exp}(\boldsymbol{k},\boldsymbol{\theta}) \sim BR_{H\to\gamma\gamma_d} N_i^{sig}(\boldsymbol{\theta}) + k_{VV\gamma} N_i^{VV\gamma}(\boldsymbol{\theta}) + \sum_{bkg \neq VV\gamma} N_i^{bkg}(\boldsymbol{\theta})$
- $N_i^{sig/bkg} = n_i^{sig/bkg} \prod_{j \in syst} (1+\theta_j \Delta_j)$ with Δ_j the value of the relative systematic uncertainty and $n_i^{sig/bkg}$ the central value from MC or from data-driven estimates
- $G(\theta_j|0,1)$: Gaussian with $\mu = 0$ and $\sigma = 1$
- **Systematic uncertainties:**
  - Experimental: from detector resolution, inefficiencies and mismeasurements
  - Theoretical: from MC samples production

Fit strategy and statistical model

Binned maximum likelihood fit on BDT score distributions with $BR(H \to \gamma\gamma_d)$ as **parameter of interest**

6 background templates (one for each background category) + signal

Uncertainties included in the fit as **nuisance parameters (NP) $\boldsymbol{\theta}$**:

$$\mathcal{L}(data|\boldsymbol{k},\boldsymbol{\theta}) = \prod_{i \in BDT_{bins}+CR_{VV\gamma}} Pois(N_i^{data}|N_i^{exp}(\boldsymbol{k},\boldsymbol{\theta})) \times \prod_{j \in syst} G(\theta_j|0,1)$$

- $\boldsymbol{k} = [BR_{H\to\gamma\gamma_d}, k_{VV\gamma}]$
- $N_i^{exp}(\boldsymbol{k},\boldsymbol{\theta}) \sim BR_{H\to\gamma\gamma_d} N_i^{sig}(\boldsymbol{\theta}) + k_{VV\gamma} N_i^{VV\gamma}(\boldsymbol{\theta}) + \sum_{bkg \neq VV\gamma} N_i^{bkg}(\boldsymbol{\theta})$
- $N_i^{sig/bkg} = n_i^{sig/bkg} \prod_{j \in syst} (1+\theta_j \Delta_j)$ with Δ_j the value of the relative systematic uncertainty and $n_i^{sig/bkg}$ the central value from MC or from data-driven estimates
- $G(\theta_j|0,1)$: Gaussian with $\mu = 0$ and $\sigma = 1$
- **Systematic uncertainties:**
  - Experimental: from detector resolution, inefficiencies and mismeasurements
  - Theoretical: from MC samples production

Background-only fit:

- Binned maximum-likelihood fit on SR+CR, assuming no signal

Exclusion fit:

- Binned maximum-likelihood fit on SR+CR, with $BR(H \to \gamma\gamma_d)$ as POI

Fit Validation

Two step validation on data

$\Longrightarrow$ **cross-check the fitting procedure in regions with low signal contamination**

1) low E_T^{miss} Validation region (VR):

- same kinematics used for the SR except for E_T^{miss}

40 GeV $< E_T^{miss} <$ 60 GeV

2) Signal Region (limited to BDT<0.5):

- same kinematics used for the SR

$E_T^{miss} >$ 60 GeV

Pre-fit

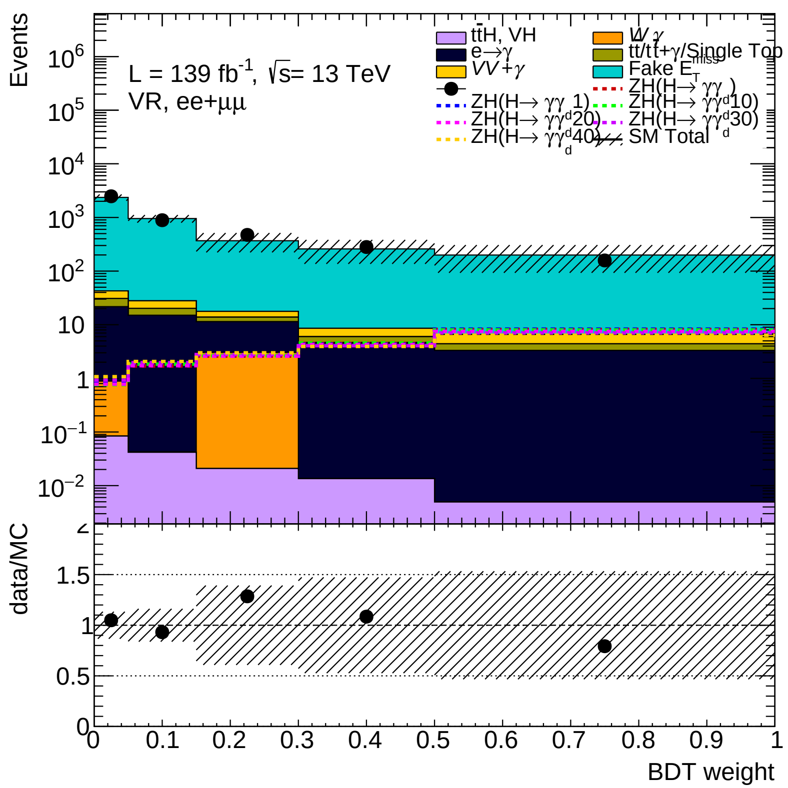

Pre-fit

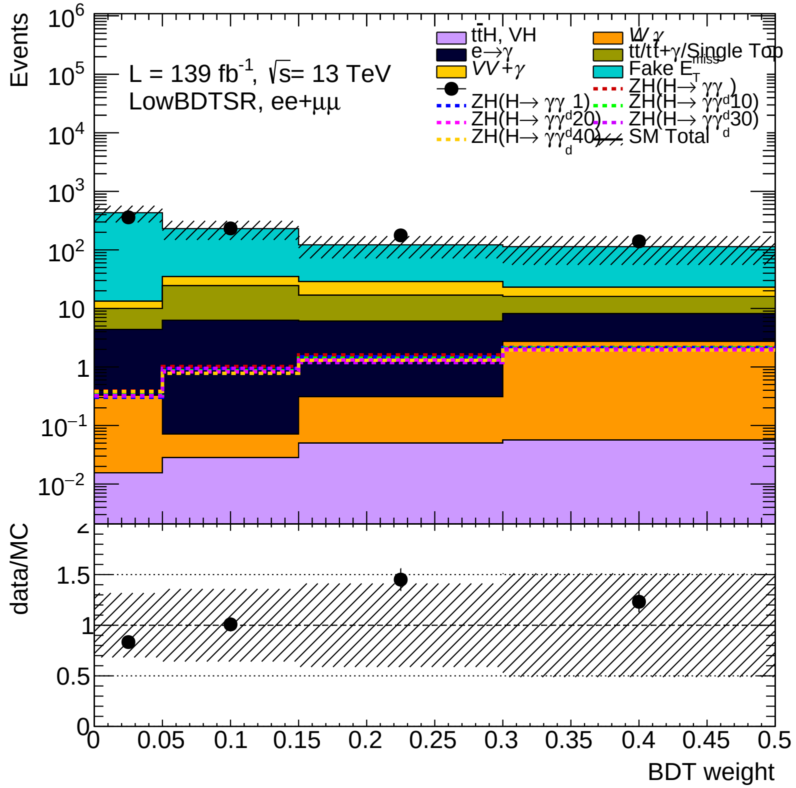

Fit Validation

Two step validation on data

$\Longrightarrow$ **cross-check the fitting procedure in regions with low signal contamination**

1) low E_T^{miss} Validation region (VR):

- same kinematics used for the SR except for E_T^{miss}

40 GeV $< E_T^{miss} <$ 60 GeV

2) Signal Region (limited to BDT$<$0.5):

- same kinematics used for the SR

$E_T^{miss} >$ 60 GeV

No discrepancies $\Longrightarrow$ **background is well modeled**

Post-fit

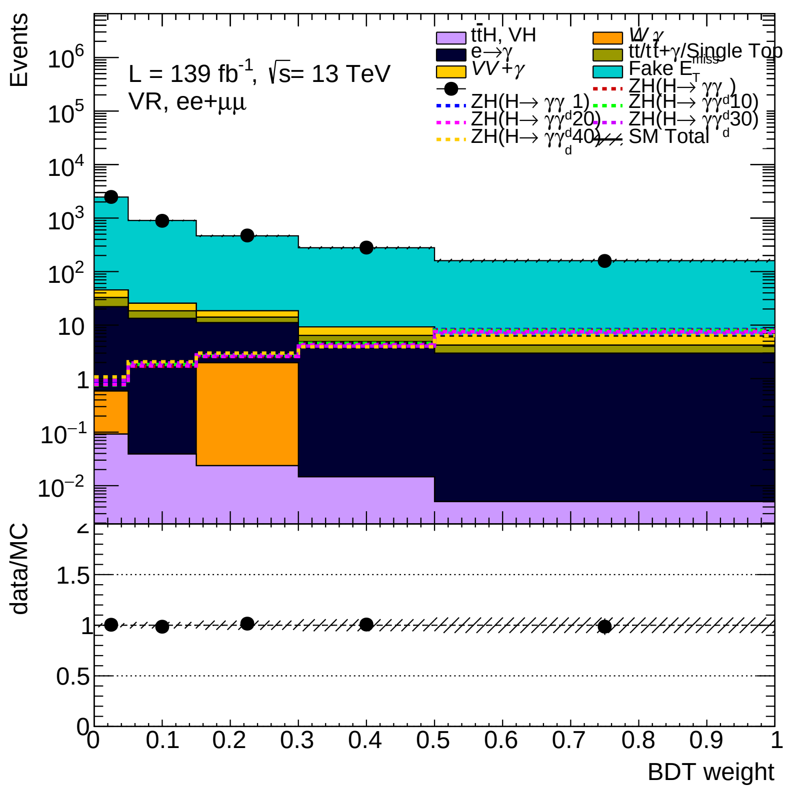

Post-fit

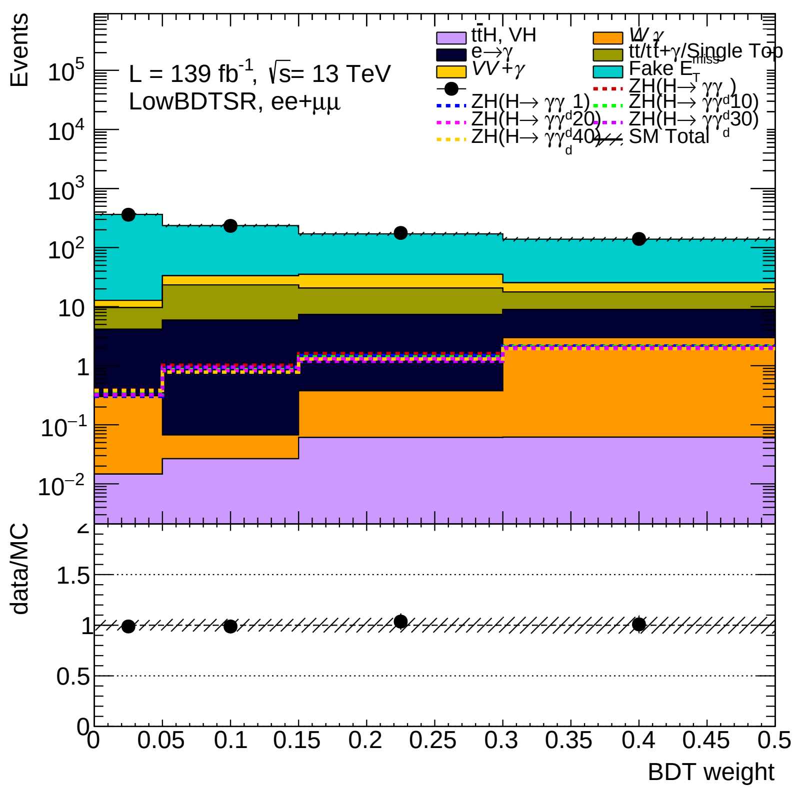

Fit Validation: Z+jets shape

Two step validation on data

$\Longrightarrow$ **cross-check the fitting procedure in regions with low signal contamination**

Z+jets shape uncertainty:

- Data/bkg discrepancies arising from Low statistics in the Z+jets sample, which is a component of the fake E_T^{miss} background $\Longrightarrow$ apply Gaussian smoothing
- Add a NP ('Smooth') to specifically address this issue: uncertainty from difference between fake E_T^{miss} shape from pure MC, and shape from smoothed Z+jets

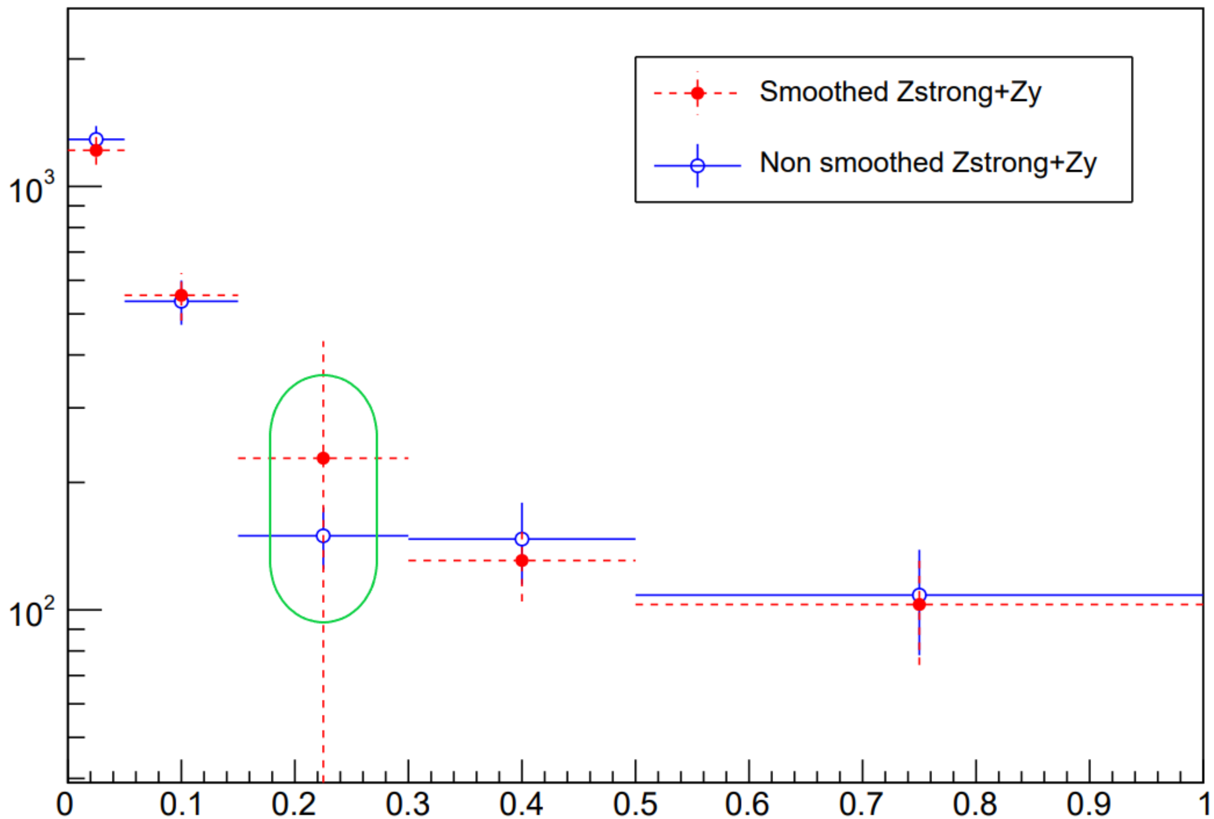

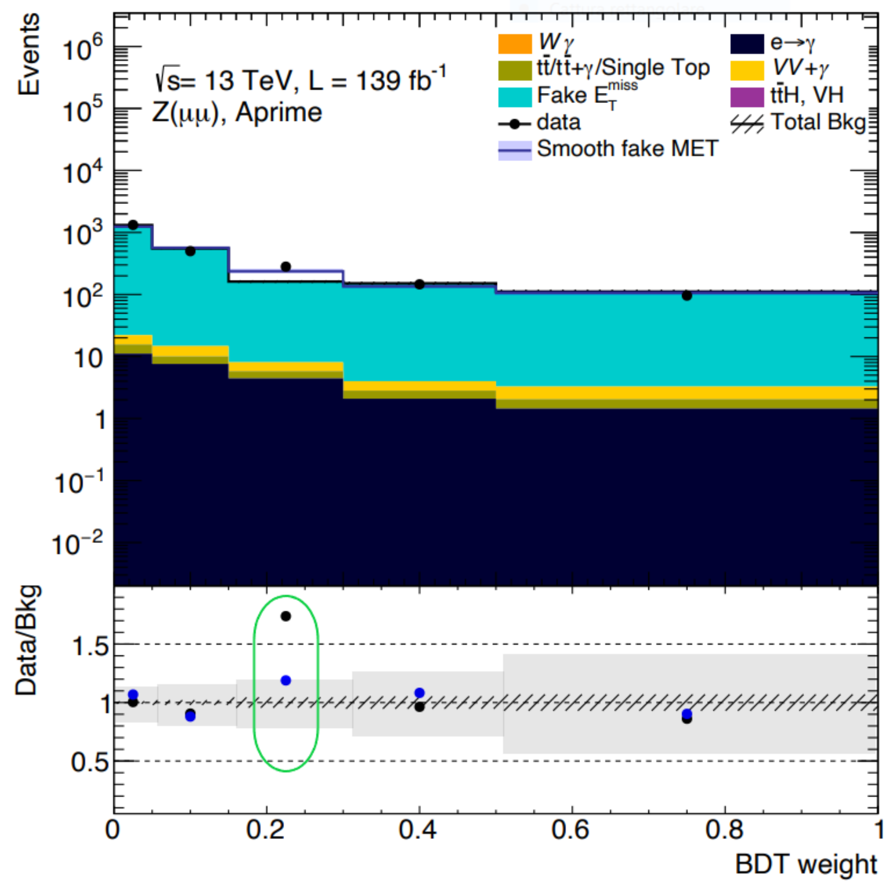

Fit Validation: ranking plots

Pre- and post-fit breakdown of systematic variations. Obtained by re-doing the fit for each systematic uncertainty by setting to constant the corresponding nuisance parameter.

Ranking plot in VR:

Ranking plot in SR (BDT $<$ 0.5):

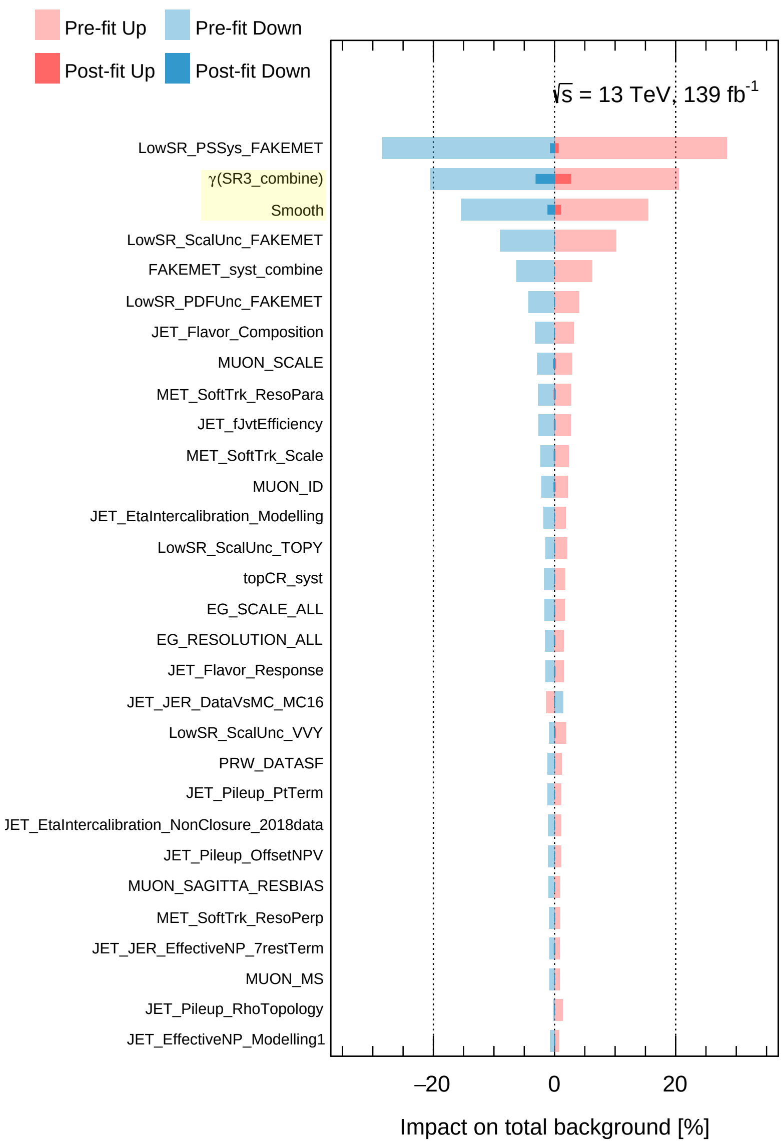

BDT binning optimization in SR

Goal: **maximise the sensitivity to γ_d signal** $\Longrightarrow$ minimise expected exclusion limits (computed with exclusion fit)

- using Asimov data-set: fictive data taken equal to pre-fit background estimate

Optimization strategy:

- Start **from 100 bins BDT** histograms
- First bin fixed to 0 - 0.5 (BDT < 0.5 used for validation)
- **Merge** the other bins, starting from highest one, **until a minimum in the expected limit is reached** $\rightarrow [0, 0.5, X^{(1)}_{min}, 1]$
- **Iterate** procedure: $[0, 0.5, X^{(n)}_{min}, \dots, X^{(1)}_{min}, 1] \Longrightarrow [0, 0.5, 0.64, 0.77, 0.88, 0.96, 1]$

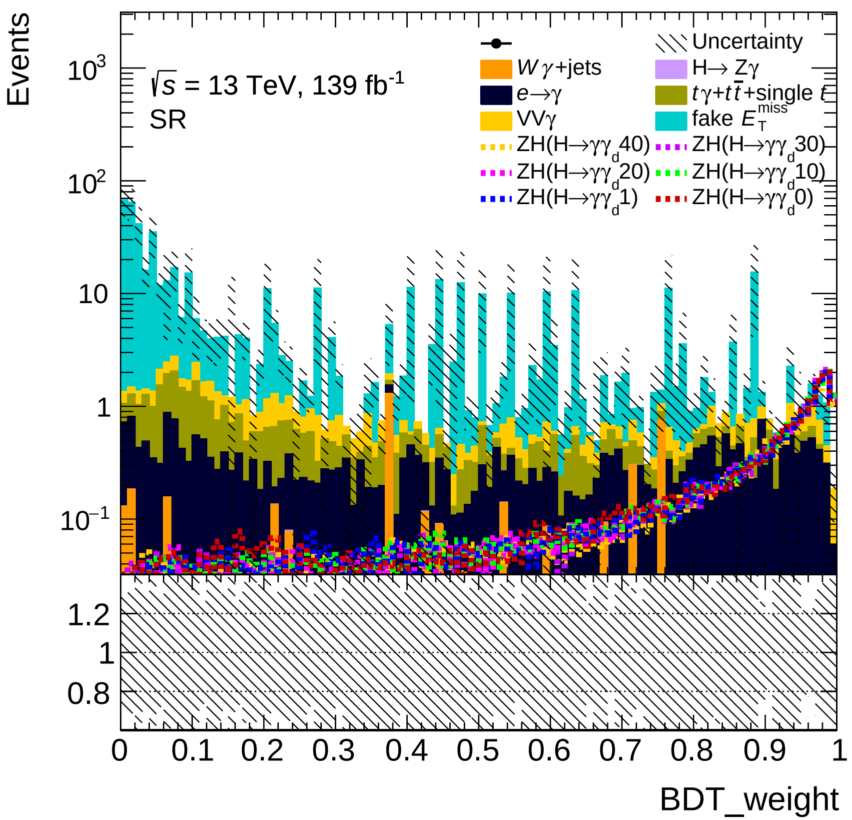

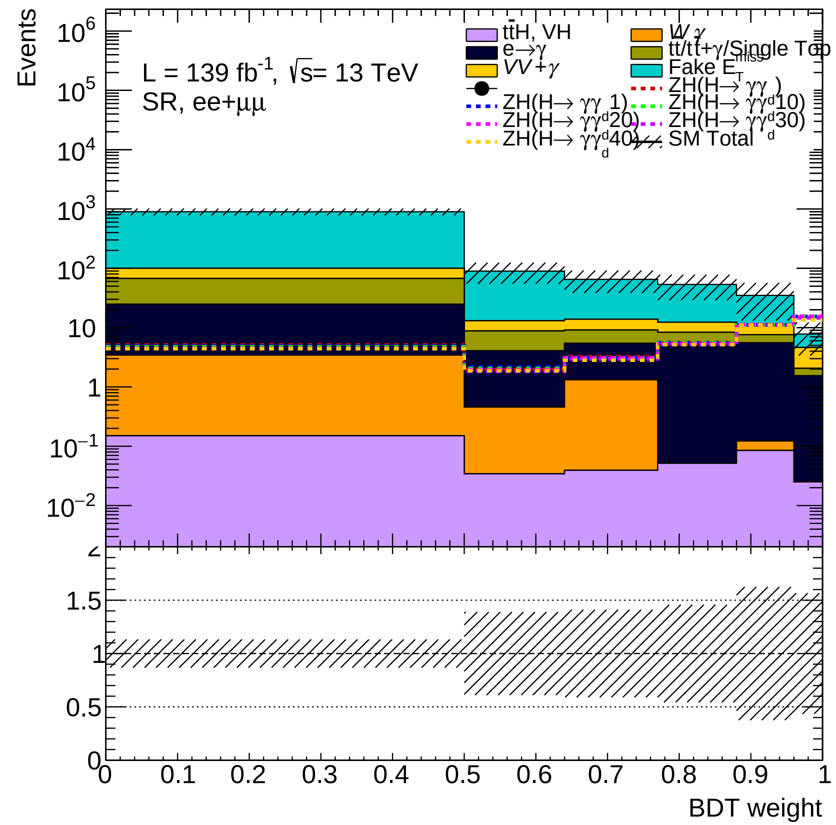

Background-only fit to data in SR

Background-only fit in SR:

- Fit to data
- $k_{VV\gamma} = 1.35 \pm 0.38$
- No excess wrt SM expectations observed

$\Longrightarrow$ **Exclusion limits can be set**

Pre-fit

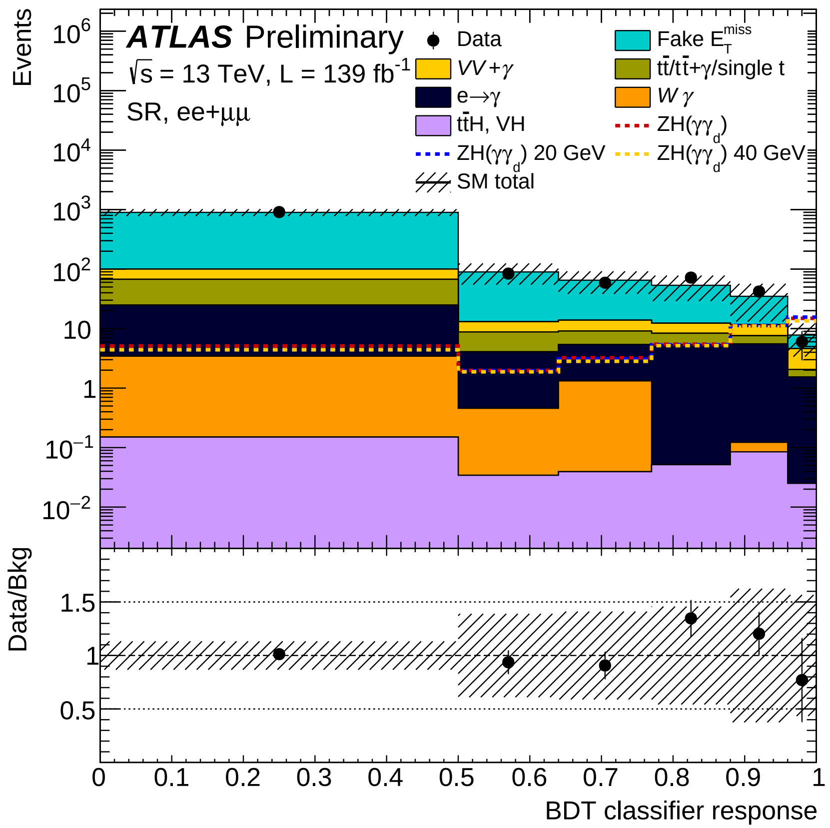

Post-fit

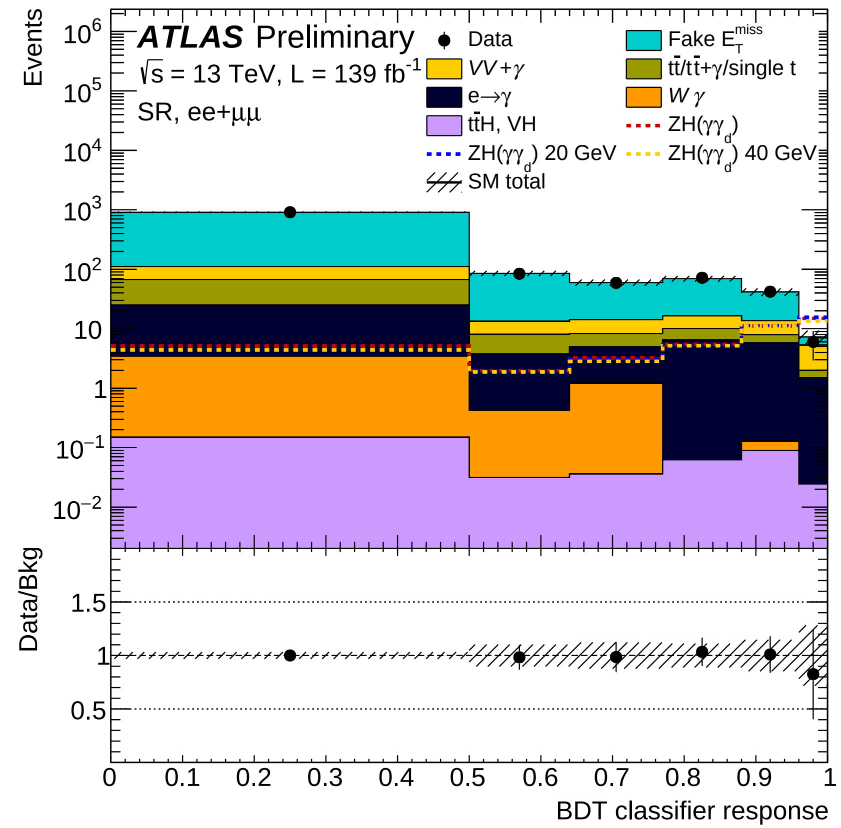

Background-only fit to data in SR

Background-only fit in SR:

- Fit to data
- $k_{VV\gamma} = 1.35 \pm 0.38$
- No excess wrt SM expectations observed

Most impactful systematics:

- Z+jets shape systematic ($\sim 21\%$)
- Statistical uncertainty ($\sim 16\%$)
- Jet energy scale and resolution ($\sim 16\%$)

$\Longrightarrow$ **Exclusion limits can be set**

BDT bin	SR 0 - 0.50	SR 0.50 - 0.64	SR 0.64 - 0.77	SR 0.77 - 0.88	SR 0.88 - 0.96	SR 0.96 - 1
Observed	**910**	**84**	**59**	**72**	**42**	**6**
Exp. SM background	$\mathbf{910 \pm 29}$	$\mathbf{85.5 \pm 8.7}$	$\mathbf{59.9 \pm 7.3}$	$\mathbf{69.7 \pm 7.8}$	$\mathbf{41.6 \pm 6.1}$	$\mathbf{7.3 \pm 2.0}$
Fake E_T^{miss}	800 ± 34	72.1 ± 8.3	45.7 ± 6.5	53.2 ± 7.1	27.9 ± 6.1	2.0 ± 1.9
$e \to \gamma$	21.5 ± 2.4	3.33 ± 0.65	3.75 ± 0.77	6.4 ± 1.2	5.7 ± 1.5	1.47 ± 0.26
$VV\gamma$	44 ± 12	5.3 ± 1.6	5.8 ± 1.7	6.4 ± 1.8	5.7 ± 1.9	3.30 ± 0.97
$t\bar{t}$, $t\bar{t}\gamma$, single t	42 ± 15	4.3 ± 1.5	3.4 ± 1.2	3.6 ± 1.2	2.13 ± 0.80	0.50 ± 0.18
$W\gamma$	3.3 ± 1.5	0.39 ± 0.18	1.18 ± 0.55	–	0.04 ± 0.02	–
$t\bar{t}H$, VH	0.15 ± 0.02	0.03 ± 0.01	0.04 ± 0.01	0.06 ± 0.01	0.09 ± 0.03	0.02 ± 0.01
Signal ($ZH \to \gamma\gamma_d$)	5.11 ± 1.34	1.98 ± 0.51	3.24 ± 1.00	5.46 ± 1.64	11.12 ± 3.06	14.87 ± 1.88

Results

Exclusion fit in SR:

- Fit to data, with $BR(H \to \gamma\gamma_d)$ as *parameter of interest*
- CLs scan to derive the 95% CL upper limit
- The exclusion limits are provided on the $BR(H \to \gamma\gamma_d)$, assuming the SM Higgs boson ZH production cross section

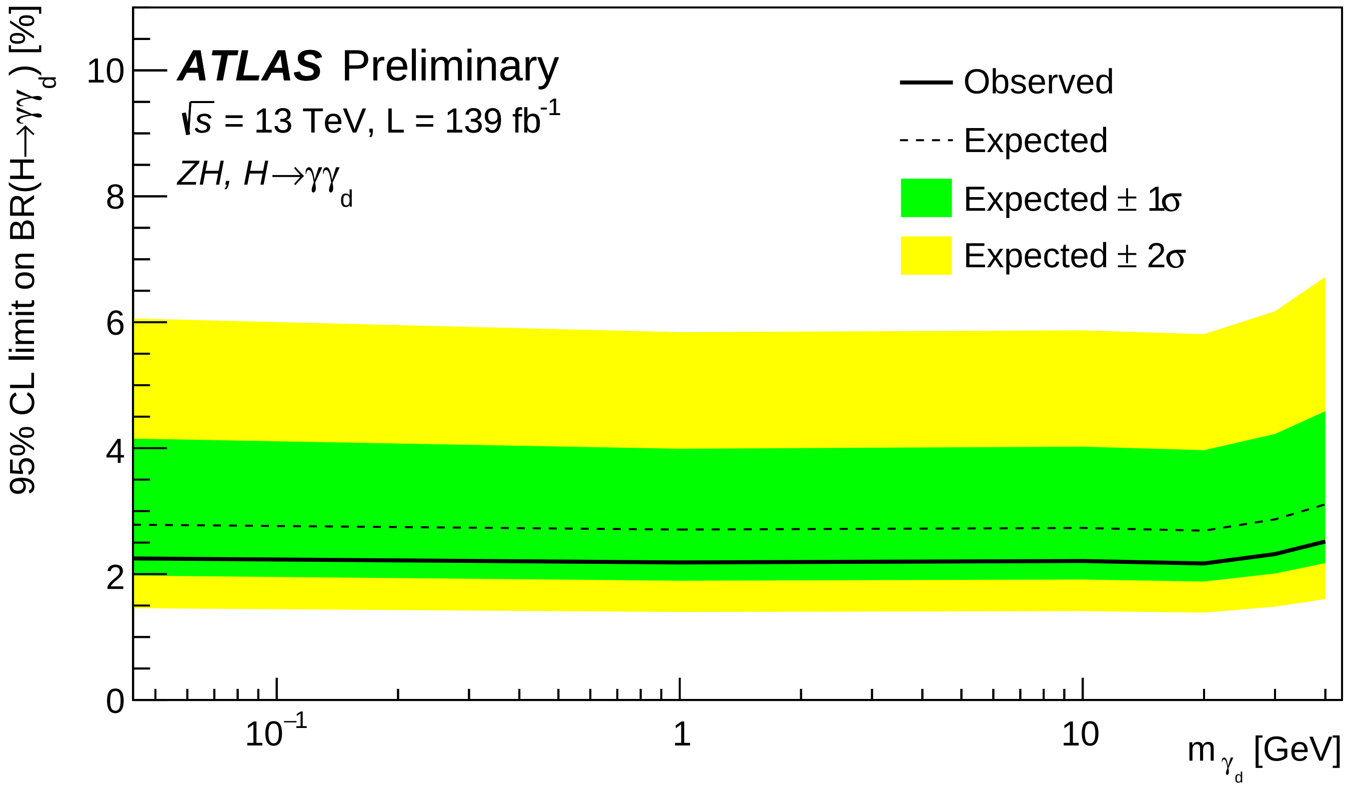

m_{γ_d} [GeV]	$BR(H \to \gamma\gamma_d)^{95}_{obs}$ [%]	$BR(H \to \gamma\gamma_d)^{95}_{exp}$ [%]
0	2.28	$2.82^{+1.33}_{-0.84}$
1	2.19	$2.71^{+1.28}_{-0.81}$
10	2.21	$2.73^{+1.31}_{-0.82}$
20	2.17	$2.69^{+1.29}_{-0.81}$
30	2.32	$2.87^{+1.36}_{-0.86}$
40	2.52	$3.11^{+1.48}_{-0.93}$

Conclusions

- A search for dark photon in the process $H \to \gamma\gamma_d$, using full Run 2 data-set, is presented (new analysis in ATLAS)
- The fit has been validated and performed to extract final results
- No excess is found $\implies$ upper limits on the $H \to \gamma\gamma_d$ branching ratio are set for dark photon masses up to 40 GeV

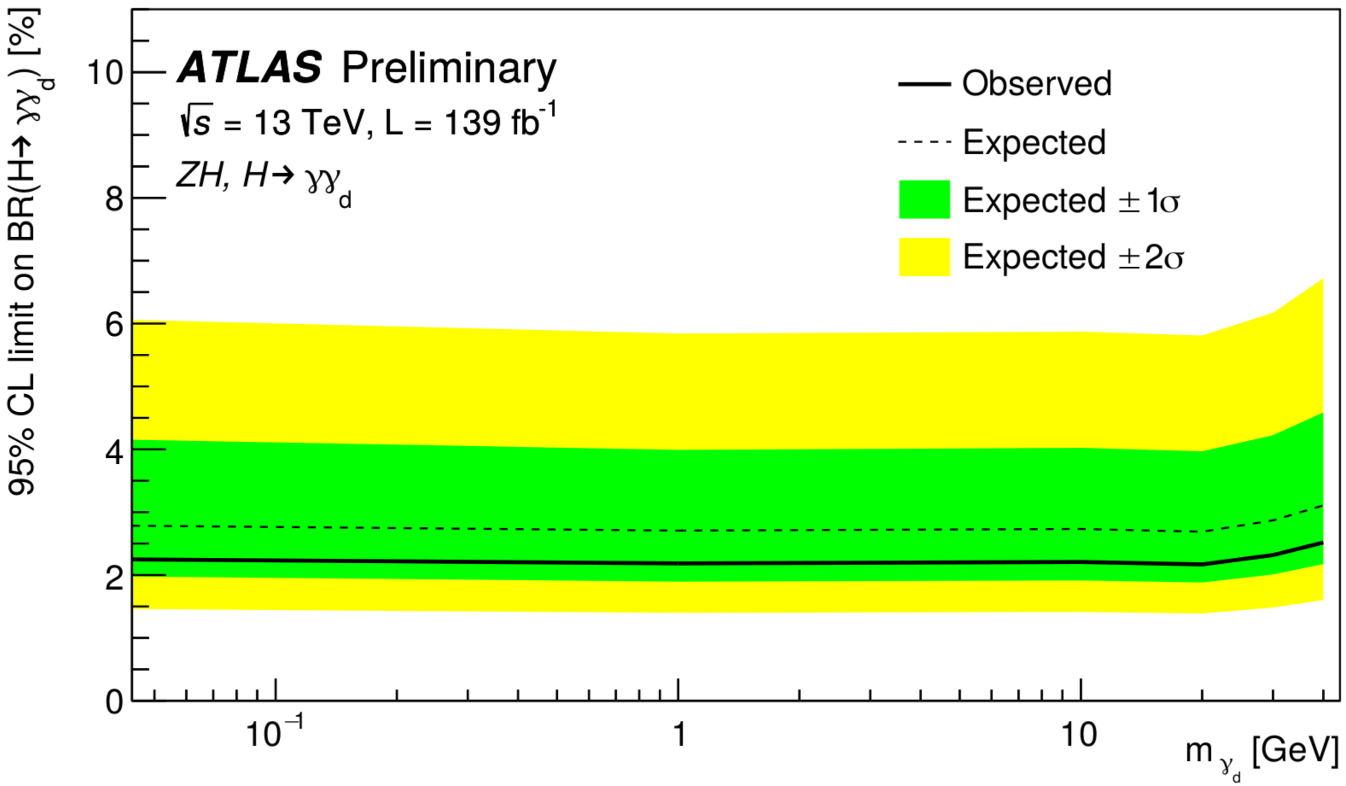

$BR(H \to \gamma\gamma_d)$	**Observed**	**Expected**
CMS	4.6%	3.6%
ATLAS	2.3%	2.8%

CMS: `http://cds.cern.ch/record/2674966`

Results are public and a Paper will soon be published by the ATLAS collaboration $\implies$ best limits at LHC for this search

`https://atlas.web.cern.ch/Atlas/GROUPS/PHYSICS/CONFNOTES/ATLAS-CONF-2022-064/ATLAS-CONF-2022-064.pdf`

Backup

Analysis selections

Medium ID, loose isolated muons. Medium ID, loose isolated electrons
Two same flavour, opposite sign ℓ, with leading $p_T > 27$ GeV, sub-leading $p_T > 20$ GeV
Veto of any additional lepton with Loose ID and $p_T > 10$ GeV
76 GeV $< m_{\ell\ell} <$ 116 GeV
One Tight ID, Tight isolated photon with $E_T^{\gamma} > 25$ GeV
$E_T^{miss} > 60$ GeV with $\Delta\phi(\vec{E}_T^{miss}, \vec{p}_T^{\ell\ell\gamma}) > 2.4$ rad
$m_{\ell\ell\gamma} > 100$ GeV
$\mathrm{N_{jet}} \leq 2$, with $p_T^{\mathrm{jet}} > 30$ GeV, $\lvert\eta\rvert < 4.5$
Veto b-jet

- AHOI (A Horrible Optimization Instrument):
  - Used to optimize the selection cuts by scanning a given optimization metric (AMS)

BDT training

- Boosted Decision Tree (**BDT**):
  - **Input variables**: E_T^{miss} significance, $m_T(\gamma, E_T^{miss})$, $m_{\ell\ell}$, $m_{\ell\ell\gamma}$, p_T^{γ}, $\frac{|\vec{E}_T^{miss}+\vec{p}_T^{\gamma}|-p_T^{\ell\ell}}{p_T^{\ell\ell}}$ in order of importance
  - Optimization of BDT hyperparameters based on Randomized + Grid search
  - 5-fold cross-validation (SKLearn::StratifiedKFold)
  - MC weights handled through 'sample_weights' parameter of XGBoost classifier + 'scale_pos_weights' to re-weight the signal class (in order to reduce imbalance between signal and background statistics)
- Kolmogorov-Smirnov test implemented $\Longrightarrow$ no overtraining observed
- BDT results consistent among different dark-photon masses

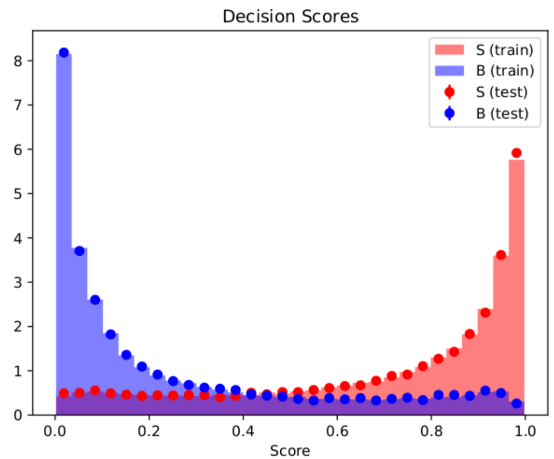

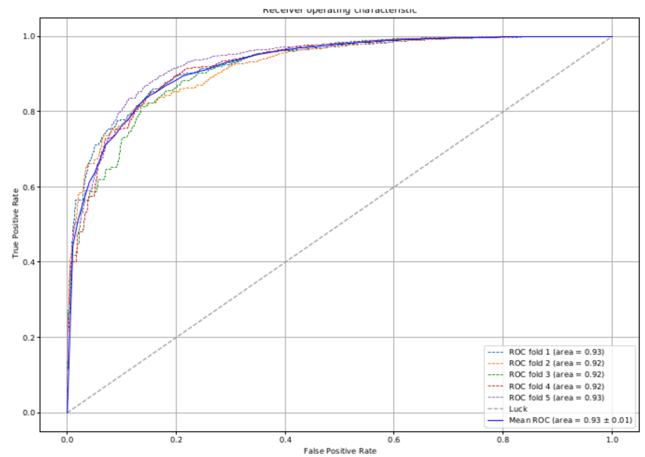

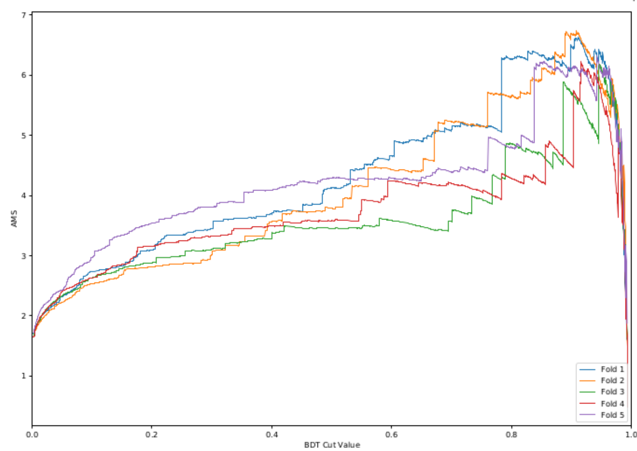

Input variables

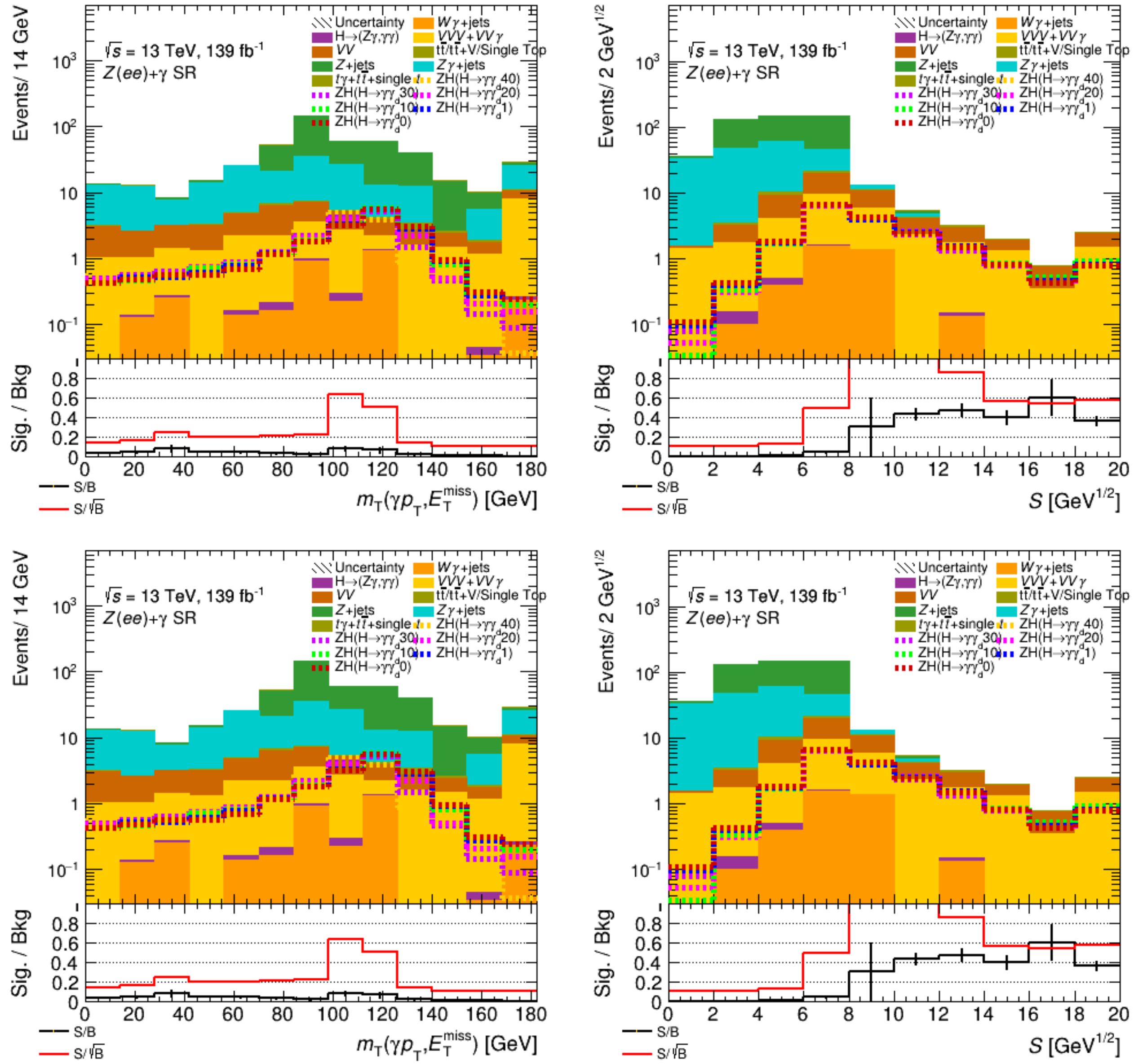

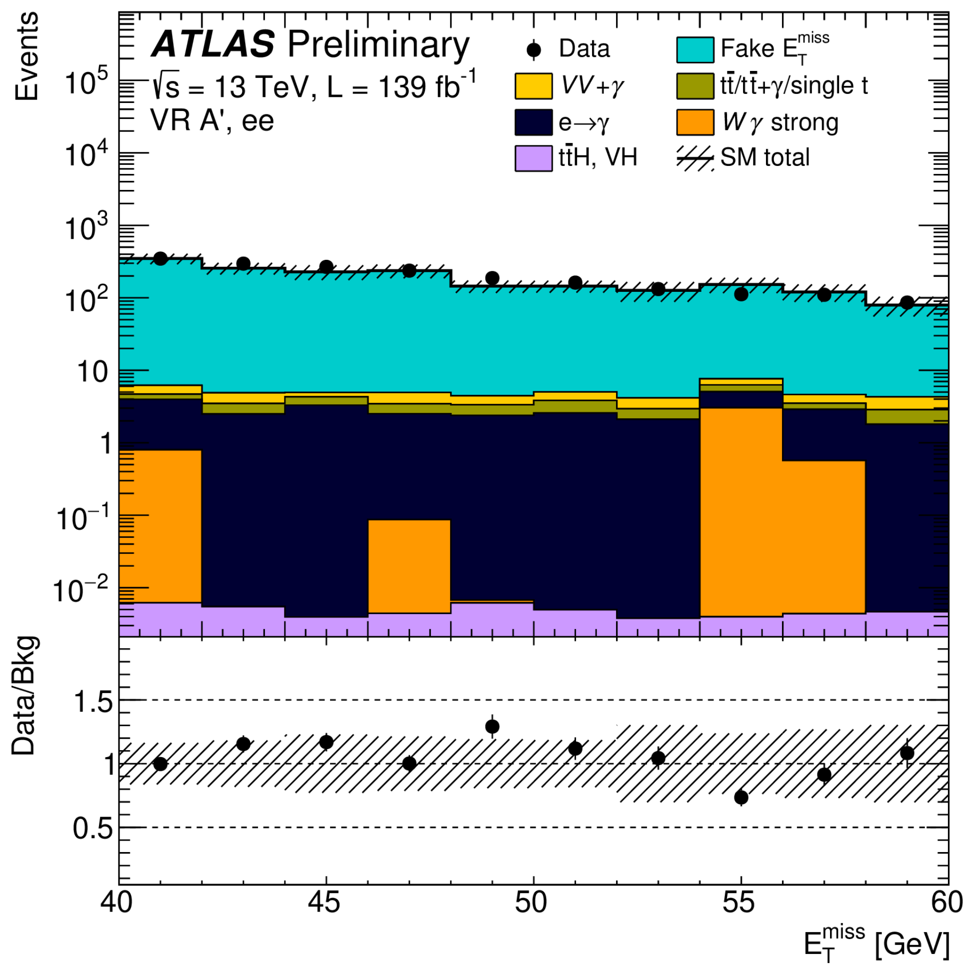
ATLAS Preliminary
√s = 13 TeV, L = 139 fb-1
VR A', ee
Data
Fake E_T^miss
VV+γ
tt̄/tt̄+γ/single t
e→γ
Wγ strong
tt̄H, VH
SM total
Events
Data/Bkg
E_T^miss [GeV]

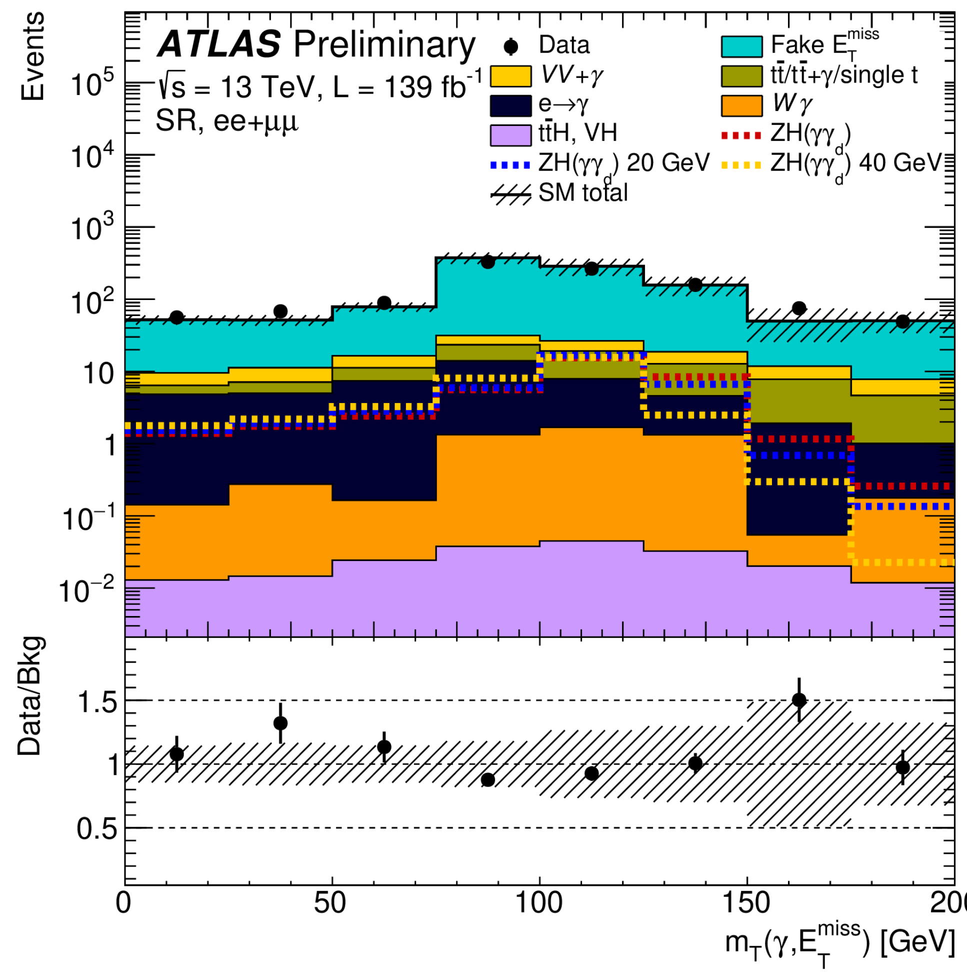
ATLAS Preliminary
√s = 13 TeV, L = 139 fb-1
SR, ee+μμ
Data
Fake E_T^miss
VV+γ
tt̄/tt̄+γ/single t
e→γ
Wγ
tt̄H, VH
ZH(γγ_d)
ZH(γγ_d) 20 GeV
ZH(γγ_d) 40 GeV
SM total
Events
Data/Bkg
m_T(γ,E_T^miss) [GeV]

Hyyd signal

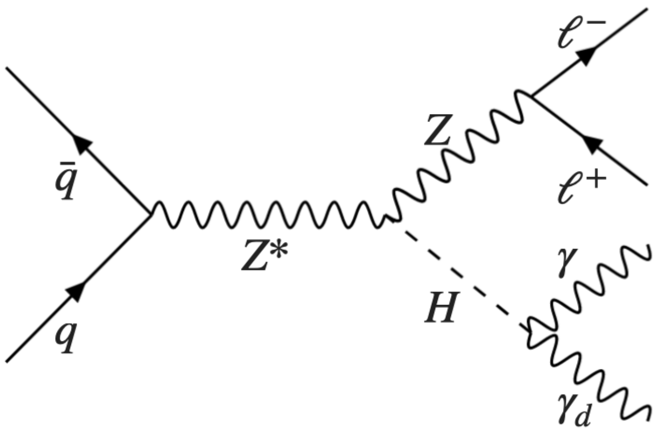

$\bar{q}$
q
Z^*
Z
H
ℓ^-
ℓ^+
γ
γ_d

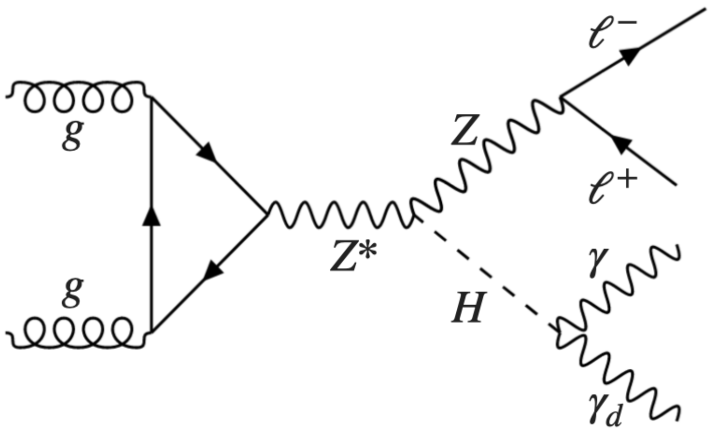

g
g
Z^*
Z
H
ℓ^-
ℓ^+
γ
γ_d

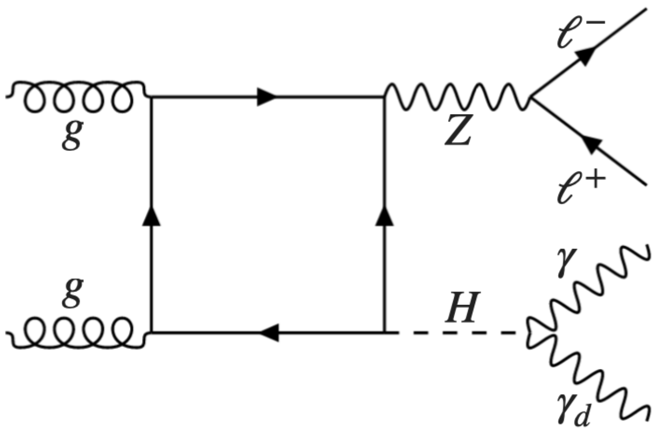

g
g
Z
H
ℓ^-
ℓ^+
γ
γ_d

Fake E_T^{miss} background

- **ABCD method**, based on E_T^{miss} and $\Delta\phi(\overrightarrow{E}_T^{miss}, \overrightarrow{p}_T^{\ell\ell\gamma})$ variable:

$$N_A^{fakeMET} = R\frac{N_B N_C}{N_D} \quad , \quad R = \frac{N_{A+A'}^{MC} N_D^{MC}}{N_{C+C'}^{MC} N_B^{MC}}$$

  - R takes into account possible correlation between the 2 variables
  - N_X is number observed data in region X, after subtraction of the contribution from non fake E_T^{miss} backgrounds

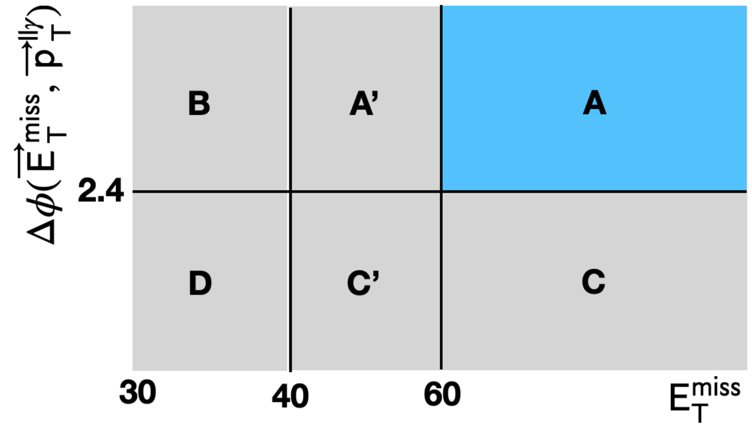

- Good stability of the R values (close to 1) for different cuts on $\Delta\phi(\overrightarrow{E}_T^{miss}, \overrightarrow{p}_T^{\ell\ell\gamma})$ and E_T^{miss}
- **Good closure in VR** (R'_{data} and R'_{MC} are consistent within uncertainties)
- The uncertainty include statistical uncertainties in the B, C and D regions and the uncertainty of R coefficient from MC statistics

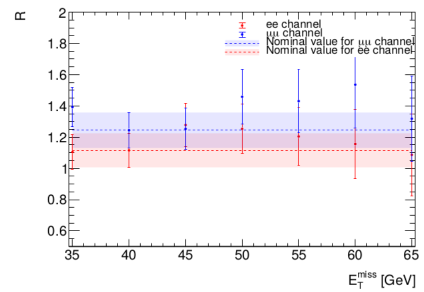

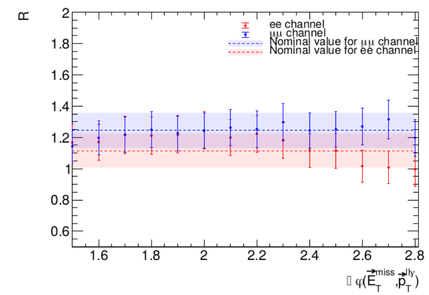

Channel	MC	Data-driven
ee	433.3 ± 56.9	413.1 ± 50.2
uu	670.8 ± 66.1	580.8 ± 64.1

Channel	R'_{MC}	R'_{data}
ee	1.094 ± 0.111	1.159 ± 0.056
uu	1.151 ± 0.111	1.181 ± 0.051

- **Probe-e CRs** defined from analysis regions (the SR and the fake E_T^{miss} ABCD regions) by replacing the photon with an extra electron
- Yields in probe-e CRs rescaled by the **fake rate** $\mathbf{F_{e\to\gamma}} = \frac{\mathbf{N_{e\gamma}}}{\mathbf{N_{ee}}}$
  - $N_{e\gamma}$ and N_{ee} from the fit of *ee* and $e\gamma$ invariant masses around Z peak
  - Signal + background model: DSCB+exp(pol3)
  - Fake rates initially inherited from mono-photon analysis, now recomputed consistently with the dark-photon anaysis selections and OR (see **Marcello's talk at the isol&fake forum** `https://atlas-glance.cern.ch/atlas/analysis/analyses/details?id=3145`)
- Subtraction of contamination from *jet* $\to$ *e* fake based on MC truth information:
  - SF=N_{true-e}/N_{tot} obtained from MC applied to data in the probe-e CRs
- Systematic uncertainties:
  - Uncertainty on the fake-rate
  - Statistics in probe-e CR
  - 100% uncertainty on the SF uncertainty for *jet* $\to$ *e* subtraction

Region	Chan	Electron faking photons
SR	$\mu\mu$	20.402 ± 0.841 ± 0.343 ± 1.405 ± 1.295
	ee	20.975 ± 0.846 ± 0.407 ± 1.466 ± 1.666

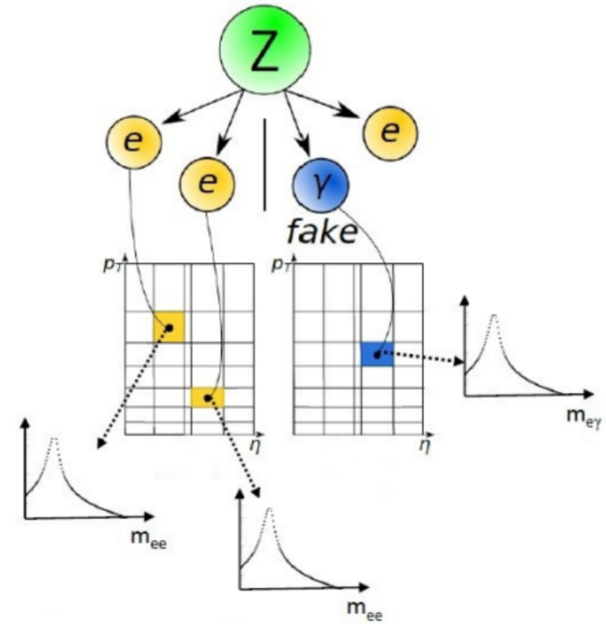

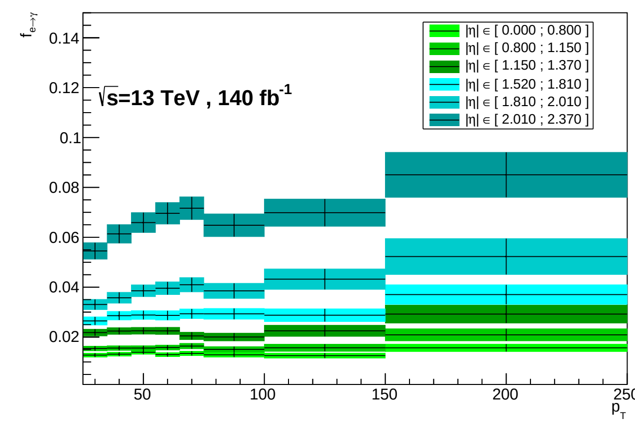

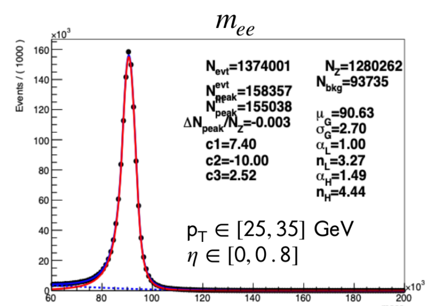

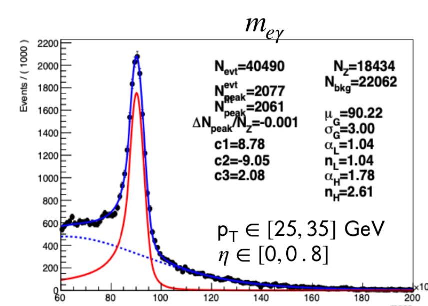

Top CR

Top background validation

- An enriched **top CR** is defined by inverting the b-jet veto and removing the cuts on $\Delta\phi(\vec{E}_T^{miss}, \vec{p}_T^{\ell\ell\gamma})$ and $m_{\ell\ell}$ to allow for more statistics
- 3 regions considered
    - Inclusive ($n_b > 0$)
    - 1 top ($n_b = 1$)
    - 2 top ($n_b = 2$)

$\Longrightarrow$ conservative **20% systematic uncertainty added to the fit**, to cover data/bkg from top CR

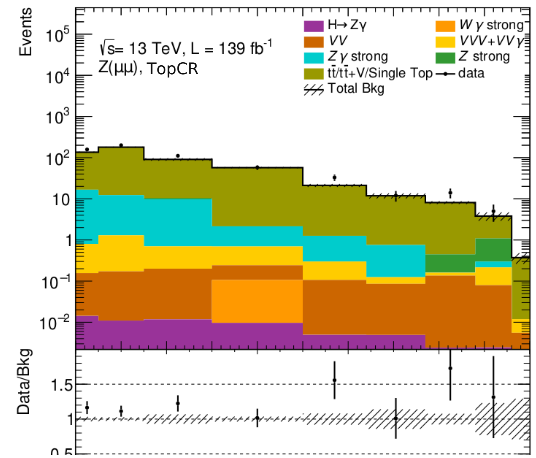

E_T^{miss} region	Top sel	Data	Tot bkg	$Z\gamma$	Z+jets	Single top	$t\bar{t}$	$t\gamma$	data/bkg
E_T^{miss} > 60 GeV	inclusive	513 ± 23	435 ± 7	18 ± 2.9	12 ± 4.9	27 ± 1.9	353 ± 3.7	21 ± 0.18	1.18 ± 0.055
E_T^{miss} > 60 GeV	1top	378 ± 19	339 ± 6.7	15 ± 2.6	12 ± 4.9	24 ± 1.8	265 ± 3.2	19 ± 0.17	1.11 ± 0.06
E_T^{miss} > 60 GeV	2top	135 ± 12	96 ± 2.3	2.8 ± 1.3	0.041 ± 0.035	2.7 ± 0.6	88 ± 1.8	1.8 ± 0.053	1.41 ± 0.13

Table 39: Yields of data and relevant backgrounds for E_T^{miss} > 60 GeV and different top categories of TopCR, ee channel. The $\Delta\phi(\vec{E}_T^{miss}, \vec{p}_T^{lly})$ and invariant mass selections are not applied, in order to increase the statistics.

E_T^{miss} region	Top sel	Data	Tot bkg	$Z\gamma$	Z+jets	Single top	$t\bar{t}$	$t\gamma$	data/bkg
E_T^{miss} > 60 GeV	inclusive	591 ± 24	508 ± 9.5	39 ± 7.7	–	35 ± 2.2	409 ± 3.9	23 ± 0.19	1.16 ± 0.05
E_T^{miss} > 60 GeV	1top	462 ± 21	393 ± 9.2	37 ± 7.6	–	30 ± 2	303 ± 3.4	21 ± 0.18	1.18 ± 0.06
E_T^{miss} > 60 GeV	2top	129 ± 11	116 ± 2.4	1.7 ± 0.88	0.4 ± 0.24	5.5 ± 0.86	106 ± 2	2.1 ± 0.056	1.11 ± 0.10

Table 40: Yields of data and relevant background for E_T^{miss} > 60 GeV and different top categories of TopCR, $\mu\mu$ channel. The $\Delta\phi(\vec{E}_T^{miss}, \vec{p}_T^{lly})$ and invariant mass selections are not applied, in order to increase the statistics.

VVy background

VVy background validation

- $3\mu + \gamma$ **VVy CR**: defined as the SR with no cuts on E_T^{miss} and $\Delta\phi(\overrightarrow{E}_T^{miss}, \overrightarrow{p}_T^{\ell\ell\gamma})$
  - Focus on $\mu\mu$ to avoid contamination from $jet \to e$
  - Dominant contribution from $e \to \gamma$ in $\mu\mu e \implies$ keep $\mu\mu\mu$
  - Too low stat with 4 leptons
- data/bkg: 1.3 ± 0.25

Lepton sel	Tot bkg	VVγ	Zγ	Z+jets	VV
inclusive	92 ± 3.9	41 ± 0.46	7.6 ± 2.7	2.8 ± 2.7	37 ± 0.61
2mu+1el	64 ± 3.6	16 ± 0.3	6 ± 2.4	3.1 ± 2.7	36 ± 0.58
3mu	24 ± 1.4	20 ± 0.34	1.6 ± 1.3	−0.25 ± 0.2	0.89 ± 0.17
4mu	2.3 ± 0.051	2.2 ± 0.047	0 ± 0	0 ± 0	0.0099 ± 0.018

Table 41: Yields of relevant backgrounds in different leptons categories of $VV\gamma$ CR. The $E_{\mathrm{T}}^{\mathrm{miss}}$ and $\Delta\phi(\vec{E}_T^{miss}, \vec{p}_T^{lly})$ selections are not applied, in order to maximize the statistics

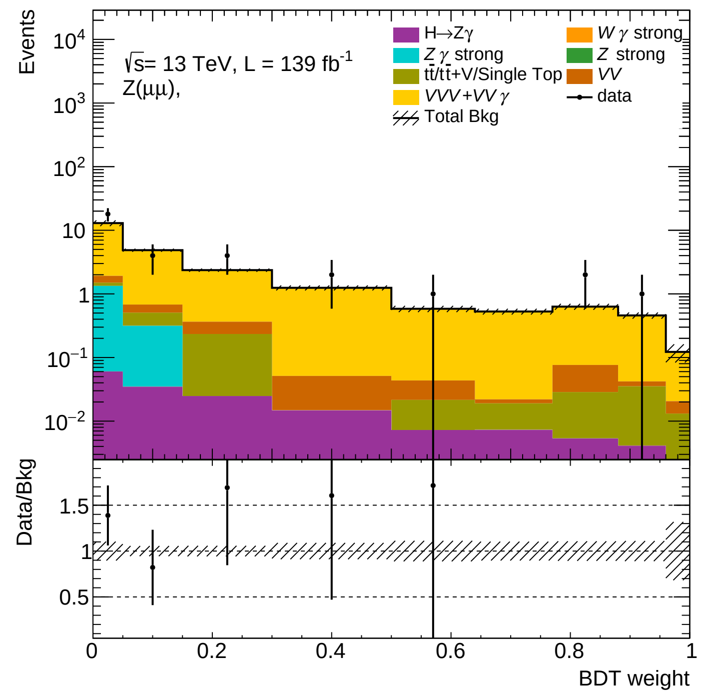

- BDT input variables distributions show good data/mc agreement

$\implies$ **VVy CR added in the fit**

Standard Model physics at the LHC

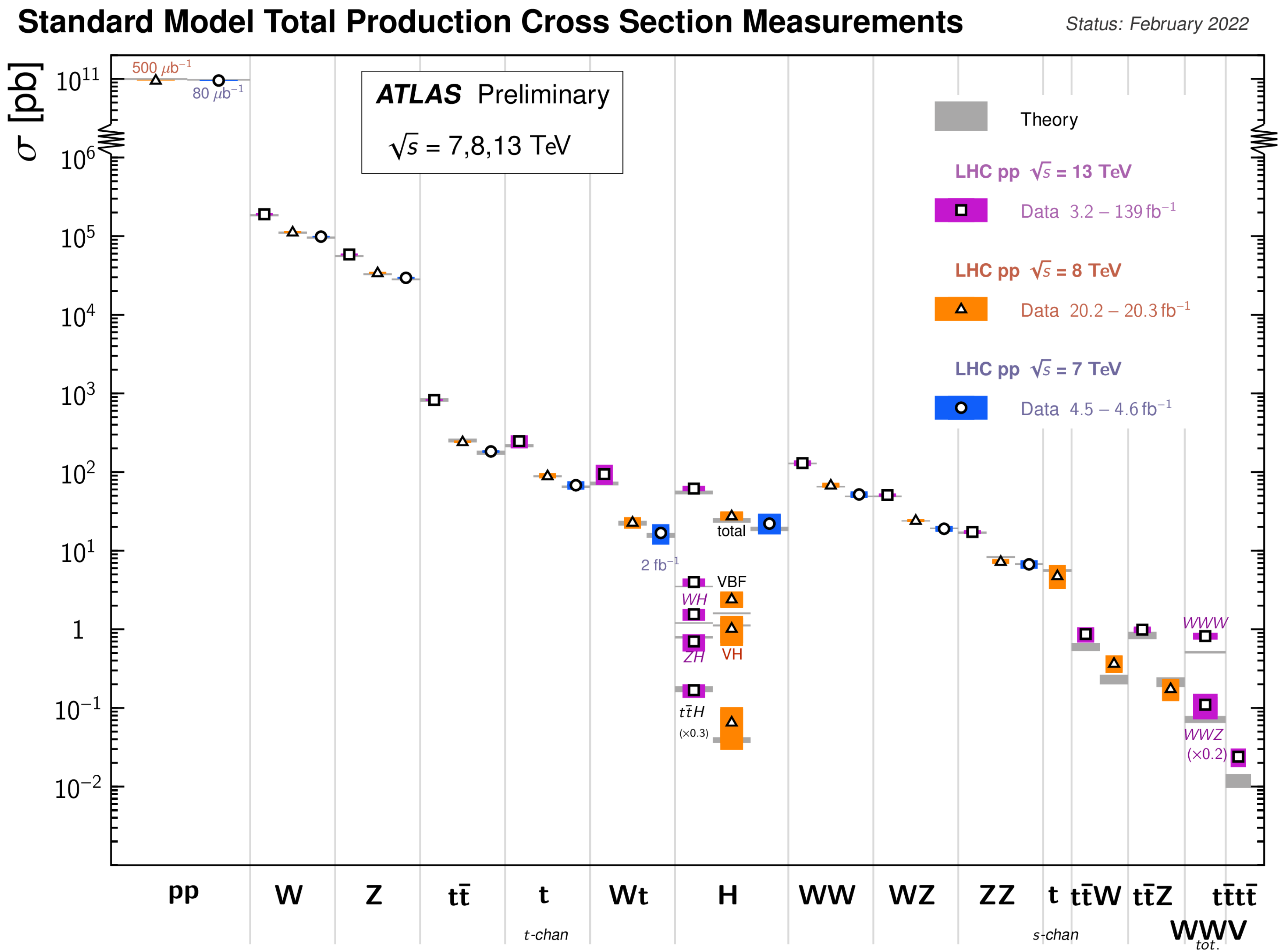

LHC / HL-LHC Plan
HiLumi
LARGE HADRON COLLIDER
LHC
HL-LHC
Run 1
Run 2
Run 3
Run 4 - 5...
LS1
EYETS
LS2
EYETS
LS3
7 TeV
8 TeV
13 TeV
13.6 TeV
13.6 - 14 TeV
energy
splice consolidation
button collimators
R2E project
cryolimit
interaction
regions
Diodes Consolidation
LIU Installation
Civil Eng. P1-P5
pilot beam
inner triplet
radiation limit
HL-LHC
installation
2011
2012
2013
2014
2015
2016
2017
2018
2019
2020
2021
2022
2023
2024
2025
2026
2027
2028
2029
2040
experiment
beam pipes
ATLAS - CMS
upgrade phase 1
ALICE - LHCb
upgrade
ATLAS - CMS
HL upgrade
75% nominal Lumi
nominal Lumi
2 x nominal Lumi
2 x nominal Lumi
5 to 7.5 x nominal Lumi
30 fb-1
190 fb-1
450 fb-1
integrated
luminosity
3000 fb-1
4000 fb-1
HL-LHC TECHNICAL EQUIPMENT:
DESIGN STUDY
PROTOTYPES
CONSTRUCTION
INSTALLATION & COMM.
PHYSICS
HL-LHC CIVIL ENGINEERING:
DEFINITION
EXCAVATION
BUILDINGS

Future perspectives at the LHC

	ZH	VBF	ggF
$\sqrt{s}$	σ		
13 TeV	0.880 pb	3.766 pb	48.61 pb
14 TeV	0.981 pb	4.260 pb	54.72 pb
27 TeV	2.463 pb	11.838 pb	146.65 pb

significance	HL-LHC (14 TeV)	HE-LHC (27 TeV)
2σ	0.012 %	0.0052 %
5σ	0.030 %	0.013 %

Experimental systematic uncertainties

Systematic uncertainty	Short description
Event	
Luminosity	uncertainty on the total integrated luminosity
PRW_DATASF	pileup profile uncertainty
Electrons	
EL_EFF_Trigger_TOTAL_1NPCOR_PLUS_UNCOR	trigger efficiency uncertainty
EL_EFF_Reco_TOTAL_1NPCOR_PLUS_UNCOR	reconstruction efficiency uncertainty
EL_EFF_ID_TOTAL_1NPCOR_PLUS_UNCOR	ID efficiency uncertainty
EL_EFF_ChargeIDSel_TOTAL_1NPCOR_PLUS_UNCOR	charge ID efficiency uncertainty
EL_EFF_Iso_TOTAL_1NPCOR_PLUS_UNCOR	isolation efficiency uncertainty
EG_SCALE_ALL	energy scale uncertainty
EG_RESOLUTION_ALL	energy resolution uncertainty
Muons	
MUON_EFF_TrigSystUncertainty MUON_EFF_TrigStatUncertainty	trigger efficiency uncertainties
MUON_EFF_RECO_STAT MUON_EFF_RECO_SYS	reconstruction and ID efficiency uncertainty for $p_T > 15$ GeV
MUON_EFF_RECO_STAT_LOWPT MUON_EFF_RECO_SYS_LOWPT	reconstruction and ID efficiency uncertainty for $p_T < 15$ GeV
MUON_EFF_ISO_STAT MUON_EFF_ISO_SYS	isolation efficiency uncertainty
MUON_EFF_TTVA_STAT MUON_EFF_TTVA_SYS	track-to-vertex association efficiency uncertainty
MUON_SCALE	energy scale uncertainty
MUON_ID	energy resolution uncertainty from inner detector
MUON_MS	energy resolution uncertainty from muon system
MUON_SAGITTA_RESBIAS	muon sagitta-related uncertainty
MUON_SAGITTA_RHO	muon sagitta-related uncertainty

- All experimental systematic uncertainties provided by PMG are included in the analysis

Systematic uncertainty	Short description
jets	
JET_EffectiveNP	energy scale uncertainty split into 15 components
JET_BJES_Response	jet-related uncertainty
JET_EtaIntercalibration_Modelling	jet-related uncertainty
JET_EtaIntercalibration_NonClosure_2018data	jet-related uncertainty
JET_EtaIntercalibration_NonClosure_highE	jet-related uncertainty
JET_EtaIntercalibration_NonClosure_negEta	jet-related uncertainty
JET_EtaIntercalibration_NonClosure_posEta	jet-related uncertainty
JET_EtaIntercalibration_TotalStat	jet-related uncertainty
JET_Flavor_Composition	jet-related uncertainty
JET_Flavor_Response	jet-related uncertainty
JET_JER_DataVsMC_MC16	jet-related uncertainty
JET_JER_EffectiveNP	jet energy resolution uncertainty split into 11 parameters
JET_JvtEfficiency	jet-related uncertainty
JET_fJvtEfficiency	jet-related uncertainty
JET_Pileup_OffsetMu	jet-related uncertainty
JET_Pileup_OffsetNPV	jet-related uncertainty
JET_Pileup_PtTerm	jet-related uncertainty
JET_Pileup_RhoTopology	jet-related uncertainty
JET_PunchThrough_MC16	jet-related uncertainty
JET_SingleParticle_HighPt	jet-related uncertainty
Flavour tagging	
FT_EFF_B_systematics	b-jet tagging efficiency
FT_EFF_C_systematics	c-jet tagging efficiency
FT_EFF_Light_systematics	light-jet tagging efficiency
FT_EFF_extrapolation	b-jet tagging efficiency with high pt extrapolation
FT_EFF_extrapolation_from_charm	c-jet tagging efficiency with high pt extrapolation
E_T^{miss}-Trigger and E_T^{miss}-Terms	
xeSFTrigWeight	trigger efficiency uncertainty
MET_SoftTrk_ResoPerp	track-based soft term related to transverse resolution uncertainty
MET_SoftTrk_ResoPara	track-based soft term related to longitudinal resolution uncertainty
MET_SoftTrk_ScaleUp	track-based soft term related to longitudinal scale uncertainty
MET_SoftTrk_ScaleDown	track-based soft term related to longitudinal scale uncertainty
Additional uncertainties on background estimations	
FAKEMET_SYST	uncertainty on the data-driven fake E_T^{miss} estimate
ELEFAKE_SYST	uncertainty on the data-driven $e \to \gamma$ estimate
Smooth	uncertainty on the shape of fake E_T^{miss} due to Z strong low statistics
TOP_SYST	uncertainty on top backgrounds normalisation from top CR

Theoretical systematic uncertainties

- Estimation of the QCD scale, PDF+α_s and Parton Shower.
- **Estimation** performed **in bins of BDT: [0, 0.5, 0.64, 0.77, 0.88, 0.96, 1]**
- Bins with zero events $\rightarrow$ use systematic from the first bin

QCD scale

Process	[0, 0.5]	[0.5, 0.64]	[0.64, 0.77]	[0.77, 0.88]	[0.88, 0.96]	[0.96, 1]
ggZHHyyd0	$^{+25.4}_{-19.2}$	$^{+25.2}_{-19.1}$	$^{+25.4}_{-19.2}$	$^{+25.6}_{-19.3}$	$^{+25.9}_{-19.5}$	$^{+25.7}_{-19.4}$
qqZHHyyd0	$^{+4.0}_{-4.1}$	$^{+3.7}_{-3.9}$	$^{+2.8}_{-4.4}$	$^{+2.6}_{-3.6}$	$^{+2.1}_{-3.2}$	$^{+2.4}_{-3.8}$
ggZHHyyd1	$^{+25.4}_{-19.2}$	$^{+25.3}_{-19.2}$	$^{+25.4}_{-19.2}$	$^{+25.5}_{-19.3}$	$^{+25.8}_{-19.4}$	$^{+25.7}_{-19.4}$
qqZHHyyd1	$^{+4.6}_{-4.3}$	$^{+3.4}_{-4.1}$	$^{+2.7}_{-4.4}$	$^{+3.1}_{-4.5}$	$^{+2.4}_{-3.8}$	$^{+2.5}_{-4.1}$
ggZHHyyd10	$^{+25.6}_{-19.3}$	$^{+25.3}_{-19.2}$	$^{+25.4}_{-19.2}$	$^{+25.5}_{-19.3}$	$^{+25.9}_{-19.5}$	$^{+25.7}_{-19.4}$
qqZHHyyd10	$^{+4.7}_{-4.4}$	$^{+5.0}_{-4.3}$	$^{+3.0}_{-4.1}$	$^{+2.3}_{-3.9}$	$^{+3.5}_{-3.4}$	$^{+2.7}_{-3.7}$
ggZHHyyd20	$^{+25.5}_{-19.3}$	$^{+25.3}_{-19.1}$	$^{+25.3}_{-19.2}$	$^{+25.6}_{-19.3}$	$^{+25.9}_{-19.5}$	$^{+25.6}_{-19.3}$
qqZHHyyd20	$^{+3.9}_{-4.1}$	$^{+3.5}_{-4.1}$	$^{+3.6}_{-3.5}$	$^{+2.6}_{-3.8}$	$^{+2.7}_{-3.8}$	$^{+2.7}_{-3.7}$
ggZHHyyd30	$^{+25.4}_{-19.2}$	$^{+25.3}_{-19.2}$	$^{+25.3}_{-19.2}$	$^{+25.6}_{-19.3}$	$^{+25.9}_{-19.5}$	$^{+25.7}_{-19.4}$
qqZHHyyd30	$^{+3.2}_{-4.1}$	$^{+3.3}_{-3.7}$	$^{+3.1}_{-3.8}$	$^{+2.2}_{-3.5}$	$^{+2.9}_{-3.2}$	$^{+2.5}_{-3.7}$
ggZHHyyd40	$^{+25.3}_{-19.2}$	$^{+25.4}_{-19.2}$	$^{+25.4}_{-19.2}$	$^{+25.7}_{-19.4}$	$^{+25.9}_{-19.5}$	$^{+25.8}_{-19.4}$
qqZHHyyd40	$^{+4.2}_{-4.1}$	$^{+2.8}_{-4.0}$	$^{+2.4}_{-3.7}$	$^{+3.6}_{-3.7}$	$^{+2.3}_{-3.3}$	$^{+2.2}_{-3.0}$
VH(Zγ)	$^{+2.3}_{-2.9}$	$^{+2.4}_{-3.4}$	$^{+3.1}_{-3.8}$	$^{+3.5}_{-3.4}$	$^{+2.9}_{-3.2}$	$^{+3.9}_{-3.9}$
VVγ	$^{+19.2}_{-8.9}$	$^{+17.7}_{-6.8}$	$^{+20.8}_{-8.4}$	$^{+23.1}_{-9.6}$	$^{+14.5}_{-14.1}$	$^{+19.3}_{-7.5}$
Wγ_{ewk}	$^{+6.4}_{-7.9}$	$^{+11.3}_{-15.1}$	$^{+8.0}_{-10.5}$	$^{+0.0}_{0.0}$	$^{+16.7}_{-19.5}$	$^{+0.0}_{0.0}$
Wγ_{qcd}	$^{+26.7}_{-53.5}$	$^{+10.9}_{-1.1}$	$^{+89.0}_{-28.2}$	$^{+0.0}_{0.0}$	$^{+0.0}_{0.0}$	$^{+0.0}_{0.0}$
Wtγ	$^{+10.1}_{-8.4}$	$^{+10.3}_{-8.5}$	$^{+10.3}_{-8.5}$	$^{+10.3}_{-8.5}$	$^{+10.3}_{-8.5}$	$^{+10.4}_{-8.6}$
single Top	$^{+7.3}_{-6.9}$	$^{+0.0}_{0.0}$	$^{+0.0}_{0.0}$	$^{+0.0}_{0.0}$	$^{+0.0}_{0.0}$	$^{+0.0}_{0.0}$
ttH(Zγ)	$^{+2.3}_{-7.1}$	$^{+3.2}_{-7.7}$	$^{+3.0}_{-7.0}$	$^{+1.9}_{-5.8}$	$^{+5.8}_{-8.6}$	$^{+3.1}_{-7.9}$
ttV	$^{+26.0}_{-18.6}$	$^{+25.7}_{-18.4}$	$^{+27.0}_{-19.1}$	$^{+25.6}_{-18.2}$	$^{+25.6}_{-18.4}$	$^{+24.0}_{-17.2}$
ttbar	$^{+13.3}_{-12.2}$	$^{+17.7}_{-14.0}$	$^{+23.3}_{-17.9}$	$^{+10.1}_{-9.7}$	$^{+10.8}_{-10.1}$	$^{+0.0}_{0.0}$
Zγ_{qcd}	$^{+25.6}_{-20.0}$	$^{+19.9}_{-17.3}$	$^{+53.1}_{-7.0}$	$^{+5.9}_{-22.7}$	$^{+56.4}_{-7.7}$	$^{+11.8}_{-33.3}$
Z$_{qcd}$	$^{+2.5}_{-4.8}$	$^{+9.6}_{-3.4}$	$^{+5.5}_{-6.2}$	$^{+28.7}_{-28.1}$	$^{+16.3}_{-7.7}$	$^{+0.0}_{0.0}$
Z$_{ewk}$	$^{+5.2}_{-6.6}$	$^{+0.0}_{0.0}$	$^{+0.0}_{0.0}$	$^{+39.4}_{-24.6}$	$^{+0.0}_{0.0}$	$^{+0.0}_{0.0}$

Table 46: Difference from nominal for upper and lower bound of the scale variation uncertainties in the signal region for different process in ll channel.

PDF+α_s

Process	[0, 0.5]	[0.5, 0.64]	[0.64, 0.77]	[0.77, 0.88]	[0.88, 0.96]	[0.96, 1]
ggZHHyyd0	±1.1	±1.1	±1.1	±1.1	±1.1	±1.0
qqZHHyyd0	±1.1	±1.1	±1.1	±0.9	±0.6	±0.4
ggZHHyyd1	±1.1	±1.2	±1.1	±1.1	±1.1	±1.1
qqZHHyyd1	±1.2	±1.2	±1.0	±0.8	±0.6	±0.4
ggZHHyyd10	±1.1	±1.2	±1.1	±1.1	±1.1	±1.0
qqZHHyyd10	±1.2	±1.0	±0.9	±0.9	±0.5	±0.4
ggZHHyyd20	±1.1	±1.2	±1.1	±1.1	±1.1	±1.0
qqZHHyyd20	±1.3	±1.3	±1.0	±0.7	±0.5	±0.4
ggZHHyyd30	±1.1	±1.2	±1.1	±1.1	±1.1	±1.0
qqZHHyyd30	±1.2	±1.1	±1.0	±0.7	±0.6	±0.4
ggZHHyyd40	±1.1	±1.2	±1.1	±1.1	±1.1	±1.0
qqZHHyyd40	±1.2	±1.3	±0.9	±0.8	±0.6	±0.4
VH(Zγ)	±0.9	±0.8	±0.8	±0.5	±0.5	±0.8
VVγ	±0.5	±1.1	±1.4	±1.1	±1.4	±1.6
Wγ_{ewk}	±5.6	±7.2	±10.0	±0.0	±10.0	±0.0
Wγ_{qcd}	±9.9	±8.1	±7.2	±0.0	±0.0	±0.0
Wtγ	±0.2	±0.7	±0.8	±0.9	±0.9	±2.1
single Top	±10.0	±0.0	±0.0	±0.0	±0.0	±0.0
ttH(Zγ)	±2.1	±2.3	±2.4	±2.3	±3.0	±3.9
ttV	±0.3	±1.0	±1.1	±1.2	±1.5	±2.8
ttbar	±1.8	±3.5	±5.1	±4.0	±5.6	±0.0

Table 49: Difference from nominal for upper and lower bound of the PDF+α_s uncertainties in the signal region for different process in ll channel.

Parton Shower

Process	[0, 0.5]	[0.5, 0.64]	[0.64, 0.77]	[0.77, 0.88]	[0.88, 0.96]	[0.96, 1]
ggZHHyyd0	±144.1	±101.0	±35.9	±21.2	±0.2	±36.5
qqZHHyyd0	±2.9	±5.3	±6.0	±0.4	±2.5	±5.8
Wγ_{ewk}	±106.4	±100.0	±100.0	±0.0	±100.0	±0.0
Wγ_{qcd}	±27.9	±100.0	±48.4	±0.0	±0.0	±0.0
Wtγ	±0.1	±2.5	±0.5	±2.5	±20.1	±70.9
ttV	±2.7	±3.1	±15.8	±10.5	±4.9	±1.6
ttbar	±5.4	±43.2	±44.3	±67.9	±73.4	±0.0
Zγ_{qcd}	±0.6	±27.5	±0.4	±128.9	±40.8	±30.3
Z$_{qcd}$	±8.0	±4.0	±67.1	±21.6	±24.2	±0.0
V$\gamma\gamma$	±6.6	±84.0	±10.0	±99.0	±19.1	±46.7
Z$_{ewk}$	±137.3	±0.0	±0.0	±100.0	±0.0	±0.0
ttW	±3.6	±130.8	±10.9	±44.5	±100.0	±100.0

Table 52: Difference from nominal of the PS uncertainties in the signal region for different process in ll channel.

Smoothing of systematics

- High impact of experimental systematics due to **low statistics** (in particular in **Z+jets**) → **high fluctuations in syst variations**
  - **Smoothing** applied **using** the **TRexDefault method from the CommonSystSmoothingTool** with high tolerance (50%)
    - Merge bins until stat uncertainty goes below 50% threshold
    - Using **'353QH twice' algorithm** (Friedman in Proc.of the 1974 CERN School of Computing, Norway, 11-24 August, 1974.) to **avoid artificial flattening of uncertainties due to rebinning**

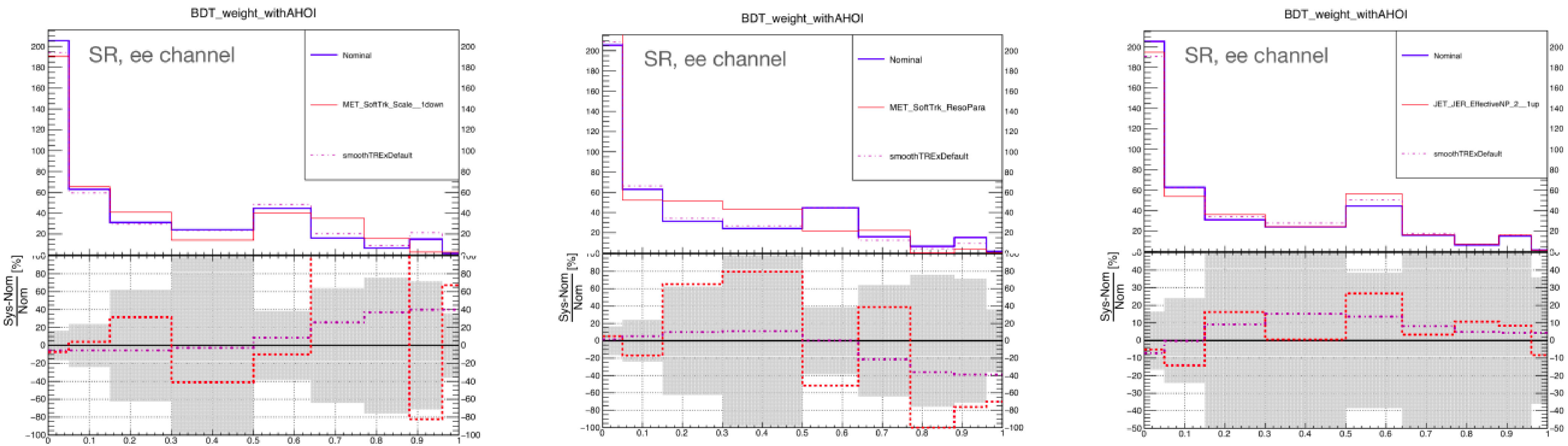

- All underconstrained NPs are characterized by up and down variations moving in the same direction in at least one bin → Solved through **symmetrization of the problematic systematics**, by taking tha maximum up or down variation.

- Experimental systematics try to "heal" data/bkg discrepancies arising from **low stat in Z strong**
- **Add a NP ('Smooth')** to specifically address this issue: uncertainty from difference between fake MET shape from pure MC, and shape from smoothed Z strong (gaussian smoothing)

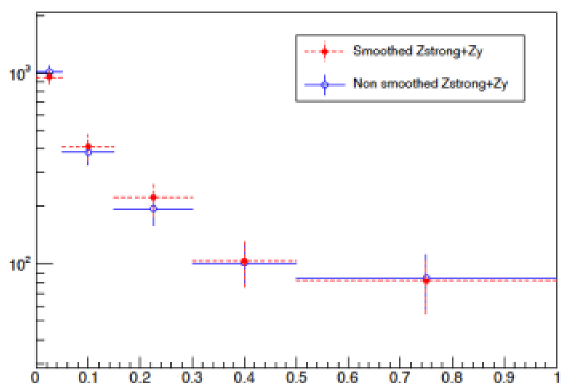

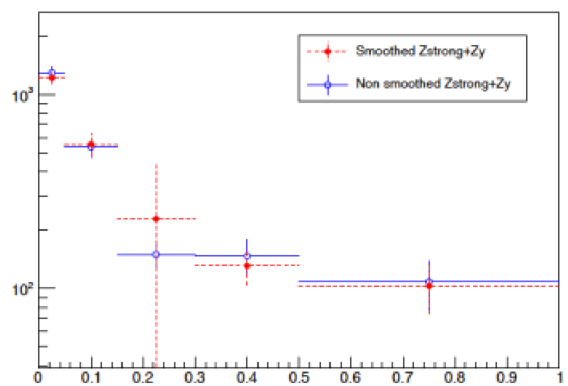

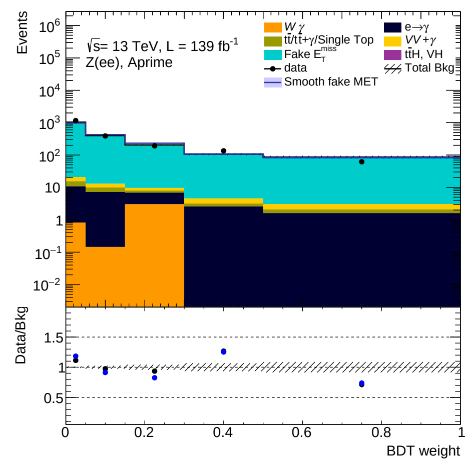

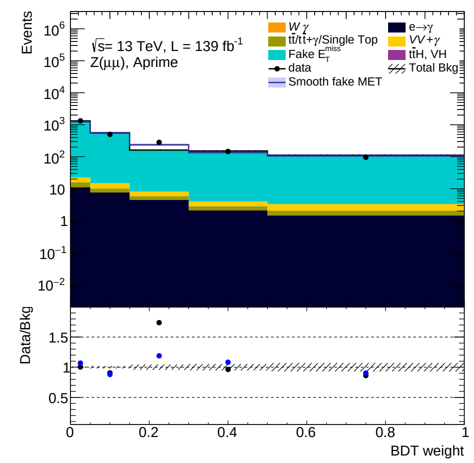

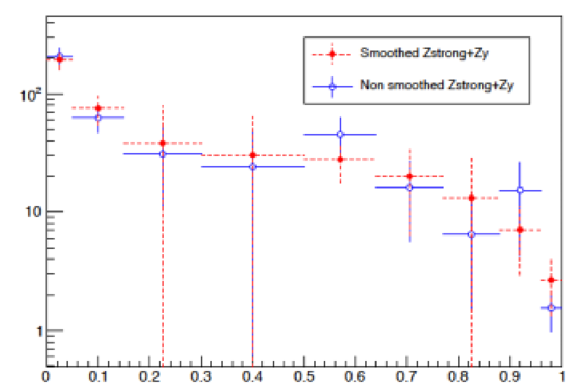

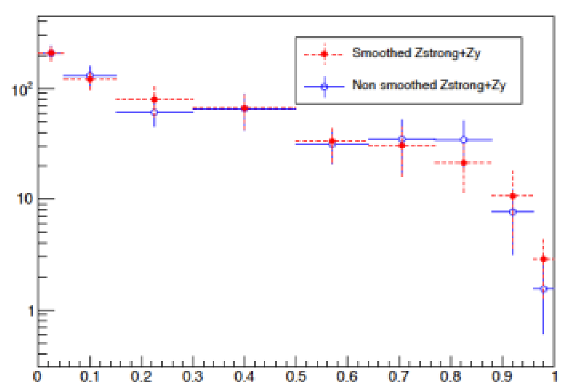

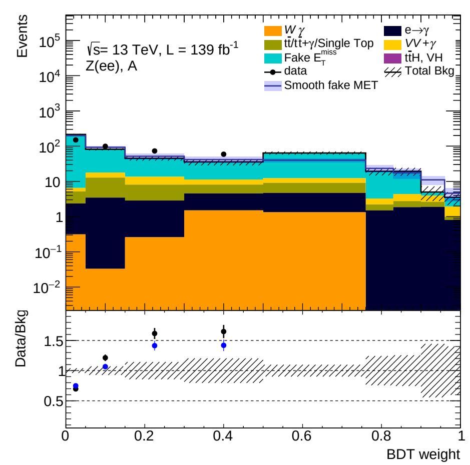

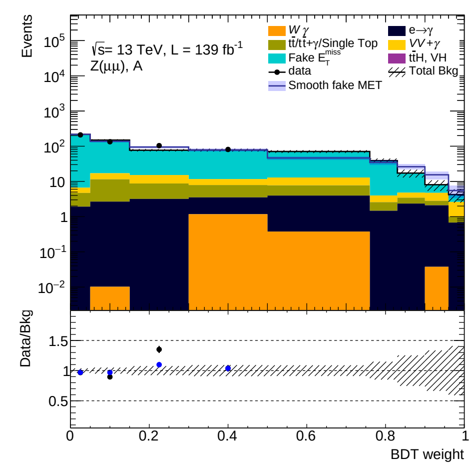

Pull plot in SR

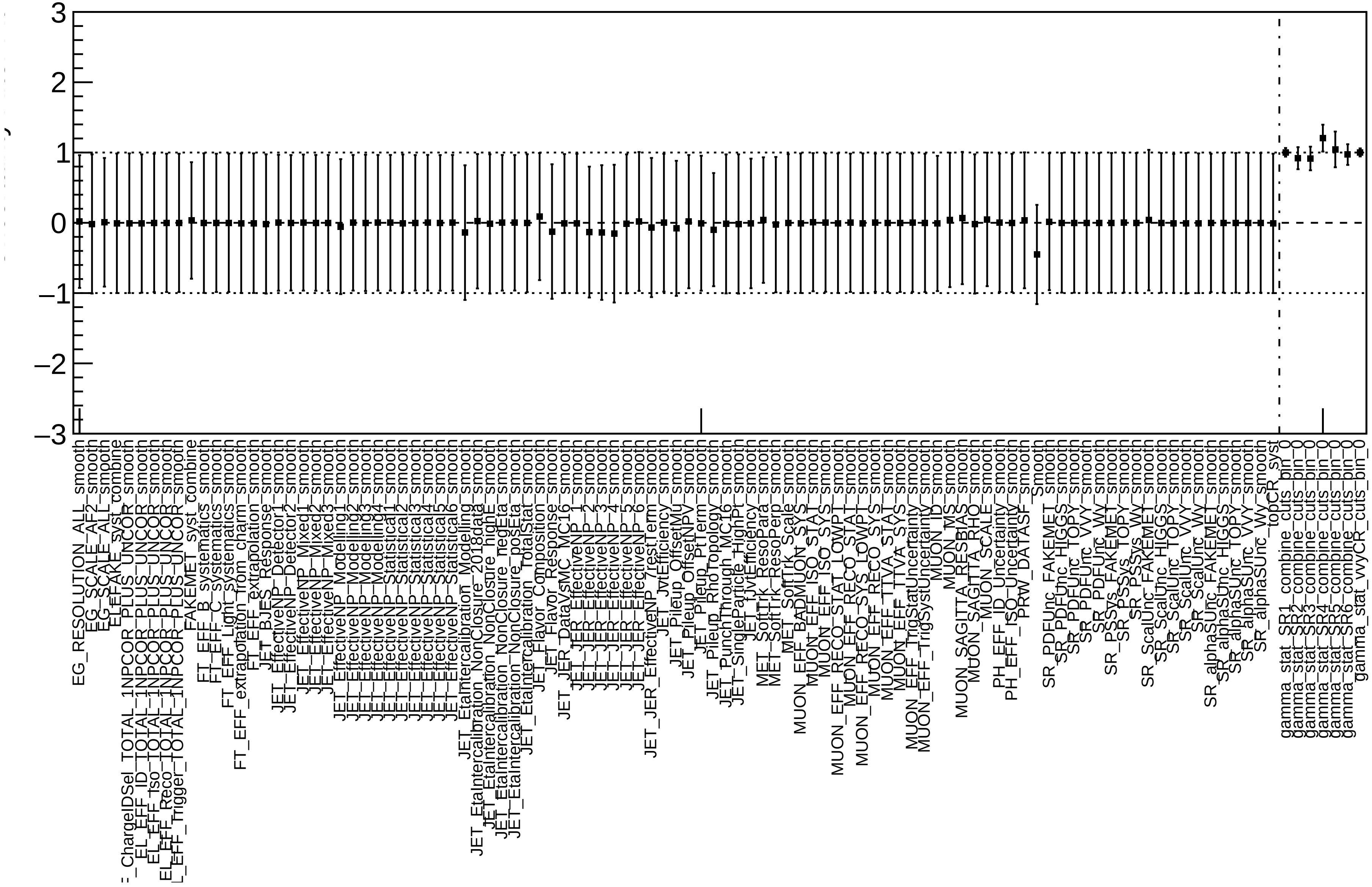

Ranking table in SR

BDT bin	0 - 0.50	0.50 - 0.64	0.64 - 0.77	0.77- 0.88	0.88 - 0.96	0.96 - 1
Total(statistical+systematic) uncertainty	3.1%	10%	12%	11%	15%	28%
Statistical uncertainty	3.1%	9.9%	12%	11%	14%	16%
Fake E_T^{miss} shape	0.17%	1.2%	0.15%	0.76%	2.4%	21%
Jet E scale and resolution	0.09%	4.3%	2.6%	1.1%	0.65%	16%
Electron, photon E scale and resolution	0.04%	0.60%	1.0%	0.21%	1.7%	7.4%
Muon E scale and resolution	0.08%	0.10%	0.28%	0.67%	1.3%	4.2%
Fake E_T^{miss} data-driven	0.52%	0.29%	0.04%	0.04%	0.29%	3.3%
E_T^{miss} soft term scale and resolution	0.27%	0.10%	0.50%	0.35%	0.33%	0.85%
Top normalization	0.07%	0.09%	0.14%	0.13%	0.07%	0.42%
Electrons faking photons data-driven	0.03%	0.10%	0.12%	0.12%	0.06%	0.34%
Reweighting of $\langle\mu\rangle$ in MC simulation	0.07%	0.09%	0.28%	0.33%	0.20%	0.23%
Flavour tagging eff.	0.02%	0.15%	0.13%	0.11%	0.07%	0.20%
Photon ID/iso/reco eff.	0.00%	0.10%	0.12%	0.11%	0.08%	0.17%
Muon trigger/ID/iso/reco eff.	0.01%	0.15%	0.10%	0.06%	0.07%	0.16%
Electron trigger/ID/iso/reco eff.	0.01%	0.18%	0.09%	0.13%	0.11%	0.15%
Theoretical top	0.09%	0.04%	0.03%	0.17%	0.17%	0.46%
Theoretical $W\gamma$	0.03%	0.13%	0.10%	0.15%	0.09%	0.44%
Theoretical $VV\gamma$	0.03%	0.10%	0.12%	0.08%	0.08%	0.35%
Theoretical Higgs	0.01%	0.10%	0.14%	0.08%	0.07%	0.22%
Theoretical fake E_T^{miss}	0.06%	0.13%	0.15%	0.28%	0.36%	0.31%

Ranking plots (asimov data-set)

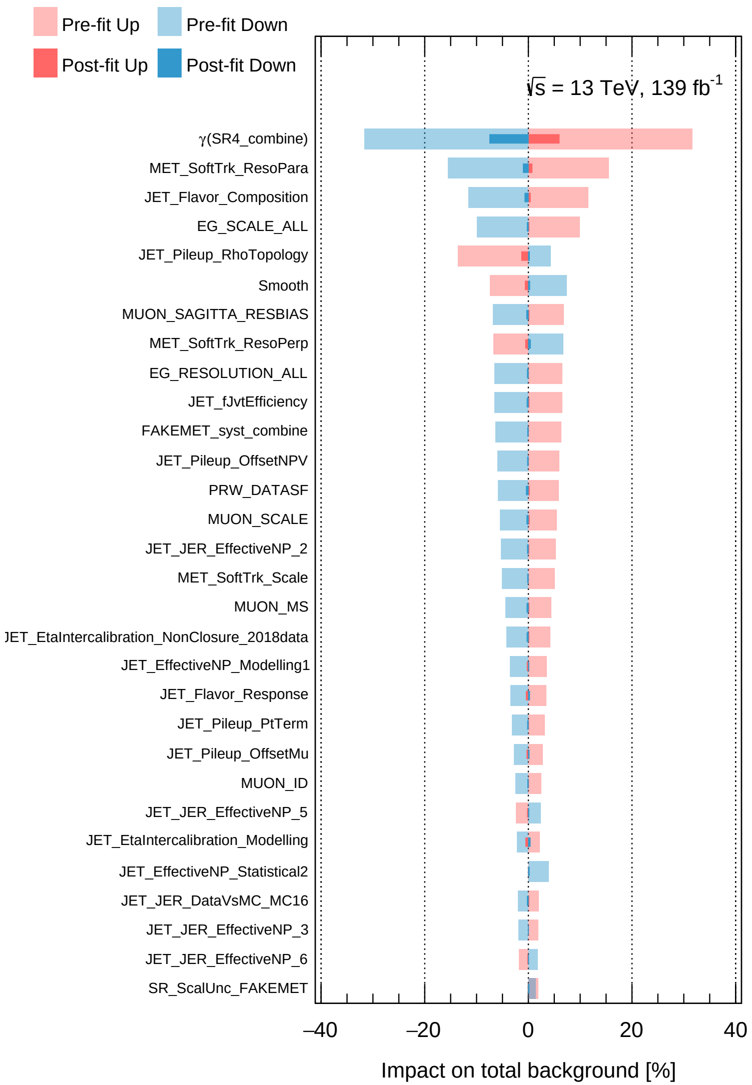

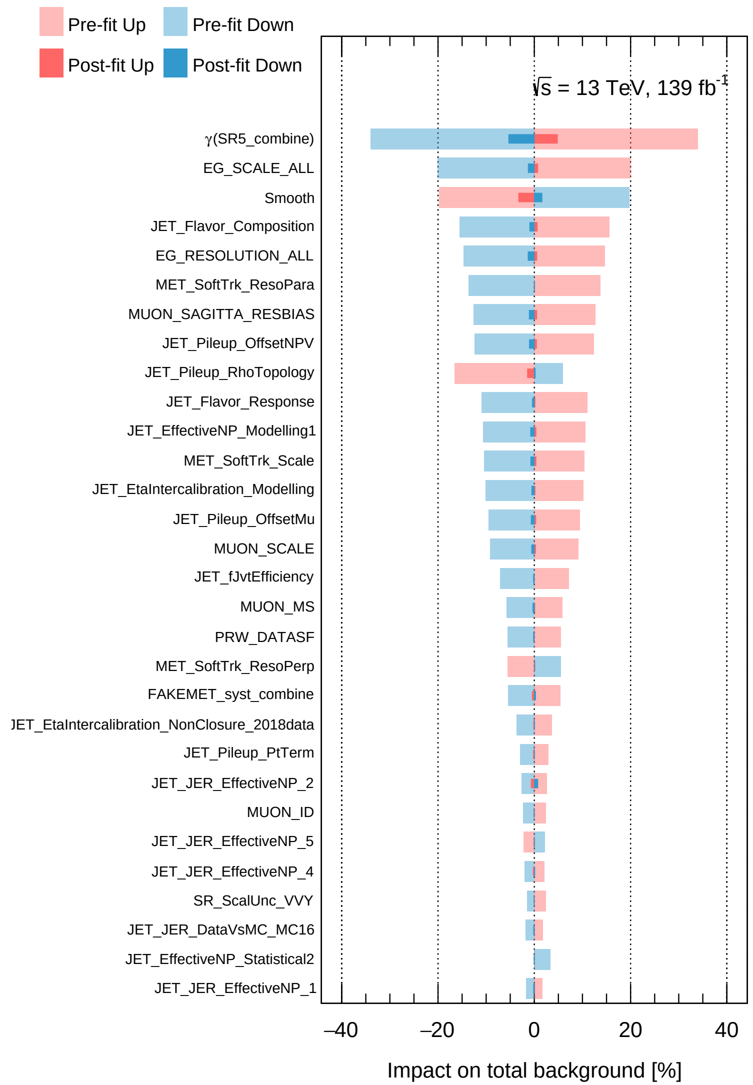

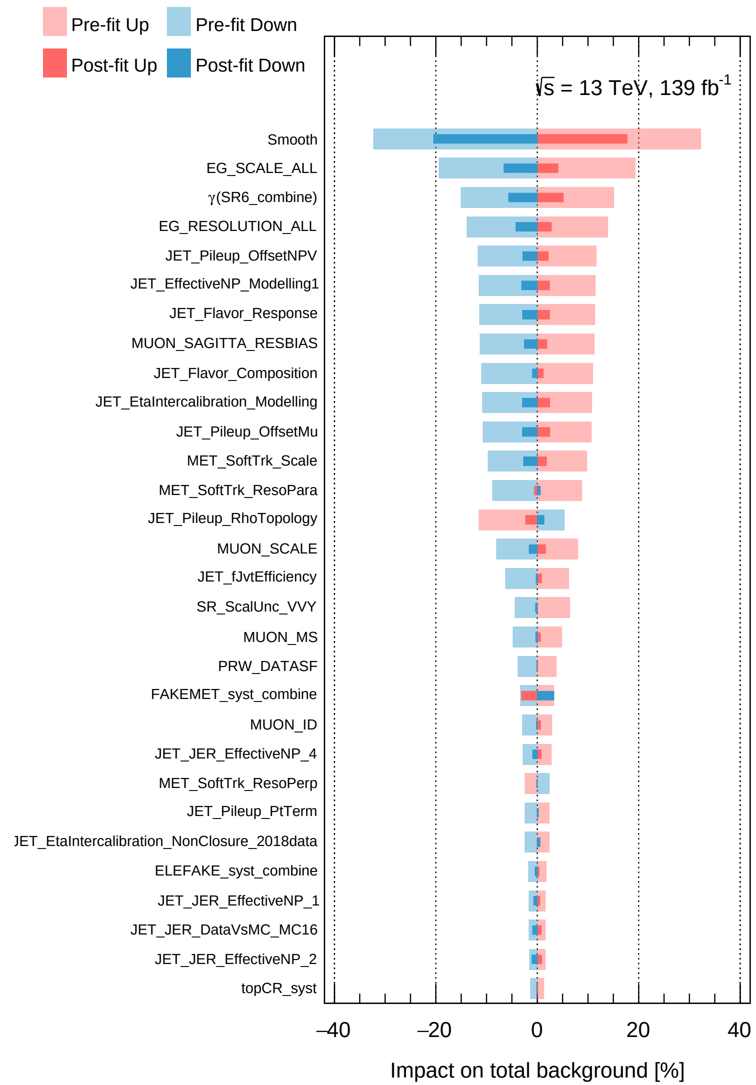

Correlation matrix in SR

	α(EG_SCALE_ALL_smooth)	α(FAKEMET_syst_combine)	α(JET_JER_EffectiveNP_2_smooth)	α(JET_JER_EffectiveNP_3_smooth)	α(MET_SoftTrk_ResoPara_smooth)	α(Smooth)	α(_SR_ScalUnc_VVY_smooth)	γ(SR1)	γ(SR2)	γ(SR3)	γ(SR4)	γ(SR5)	γ(SR6)	γ(vvyCR)	k1
α(EG_SCALE_ALL_smooth)	1.00	-0.01	-0.04	-0.02	-0.09			0.04	-0.11	0.22	-0.07	-0.19	-0.03	0.01	-0.07
α(FAKEMET_syst_combine)	-0.01	1.00	0.07	0.03	-0.21	-0.03		-0.49	-0.13	-0.04	-0.01	0.05	0.04	0.01	-0.08
_JER_EffectiveNP_2_smooth)	-0.04	0.07	1.00	-0.10	-0.05	0.12		0.18	-0.26	-0.26	-0.07	0.11	-0.02		0.08
_JER_EffectiveNP_3_smooth)	-0.02	0.03	-0.10	1.00	-0.03	0.07		0.10	-0.24	-0.18		0.10	-0.01		0.09
T_SoftTrk_ResoPara_smooth)	-0.09	-0.21	-0.05	-0.03	1.00	0.09		-0.14	-0.04	-0.31	-0.24	0.09	-0.02	0.01	0.01
α(Smooth)		-0.03	0.12	0.07	0.09	1.00	-0.01	-0.14	0.34	-0.13	0.14	0.41	-0.23	0.02	-0.06
(_SR_ScalUnc_VVY_smooth)						-0.01	1.00	0.01					-0.01		-0.48
γ(SR1)	0.04	-0.49	0.18	0.10	-0.14	-0.14	0.01	1.00		0.11	0.12	0.02	0.05	0.01	-0.06
γ(SR2)	-0.11	-0.13	-0.26	-0.24	-0.04	0.34			1.00	0.36	0.30	0.33	-0.03		-0.04
γ(SR3)	0.22	-0.04	-0.26	-0.18	-0.31	-0.13		0.11	0.36	1.00	0.31	0.04	0.06		-0.08
γ(SR4)	-0.07	-0.01	-0.07		-0.24	0.14		0.12	0.30	0.31	1.00	0.38	0.03		-0.05
γ(SR5)	-0.19	0.05	0.11	0.10	0.09	0.41		0.02	0.33	0.04	0.38	1.00	0.01		0.01
γ(SR6)	-0.03	0.04	-0.02	-0.01	-0.02	-0.23	-0.01	0.05	-0.03	0.06	0.03	0.01	1.00	0.02	-0.05
γ(vvyCR)	0.01	0.01			0.01	0.02		0.01					0.02	1.00	-0.21
k1	-0.07	-0.08	0.08	0.09	0.01	-0.06	-0.48	-0.06	-0.04	-0.08	-0.05	0.01	-0.05	-0.21	1.00

Dark photon experimental status

The most often studied mediator in recent times is kinetically-mixed dark photon, where the two gauge groups $U(1)$ and $U(1)_d$, concern the SM photon and the dark photn respectively. Focusing on the interactions with just the photon, the vacuum interactions for this portal are:

$$\mathcal{L}_0 = -\frac{1}{4}F_{\mu\nu}F^{\mu\nu} - \frac{1}{4}F_{d\mu\nu}F_d^{\mu\nu} - \frac{\epsilon}{2}F_{\mu\nu}F_d^{\mu\nu} + \frac{1}{2}m_d^2 A_{d\mu}A_d^{\mu} + eJ_\mu A^\mu + e' J_{d\mu}A_d^\mu$$

The physics arising from the Lagrangians above depends on the considered kind of dark photon:

- the *massless* kind, which does not couple directly to any of the SM currents and interacts instead with ordinary matter only through operators of dimension higher than four: a field redefinition $\hat{A}_{d\mu} = A_{d\mu} - \epsilon A_\mu$ eliminates the kinetic mixing term, leaving the following interactions

  $$\mathcal{L}_0 = -\frac{1}{4}(1-\epsilon^2)F_{\mu\nu}F^{\mu\nu} - \frac{1}{4}F_{d\mu\nu}F_d^{\mu\nu} + eJ_\mu A^\mu + e'(\hat{A}_d^\mu + \epsilon A^\mu)J_{d\mu}$$

  In the absence of a dark current J_d, we would have a completely decoupled vector $\hat{A}_d$ with no observable effects. Hence in the massless vector limit, we expect that the only limits would come from effects that involve the DM.
- the *massive* kind, which couples to ordinary matter through a current (with arbitrary charge), that is, a renormalizable operator of dimension four. The massless limit of this case does not correspond to the massless case above.

Dark photon experimental status

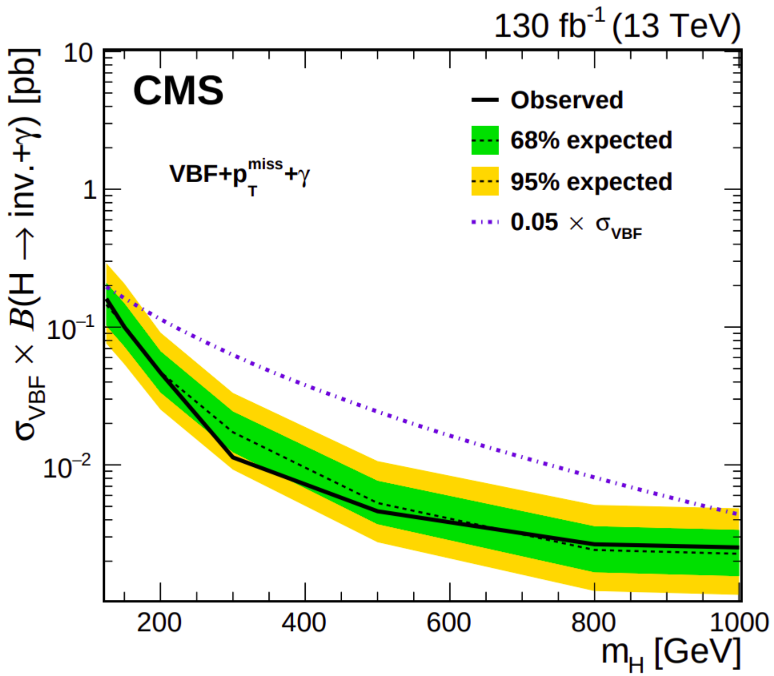

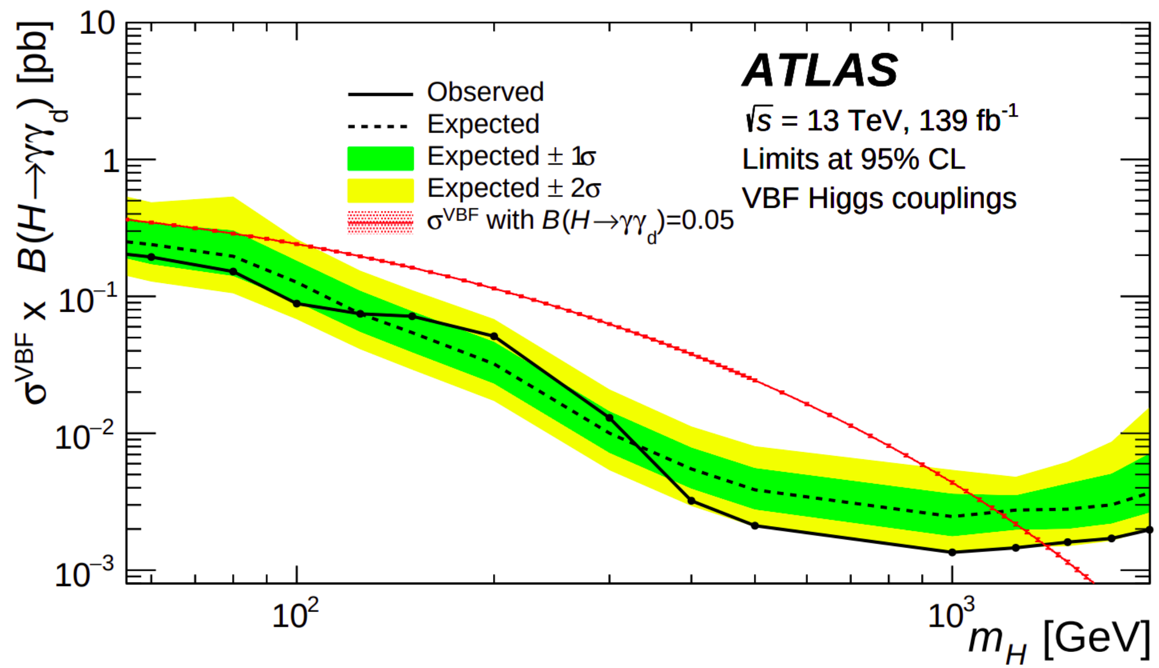

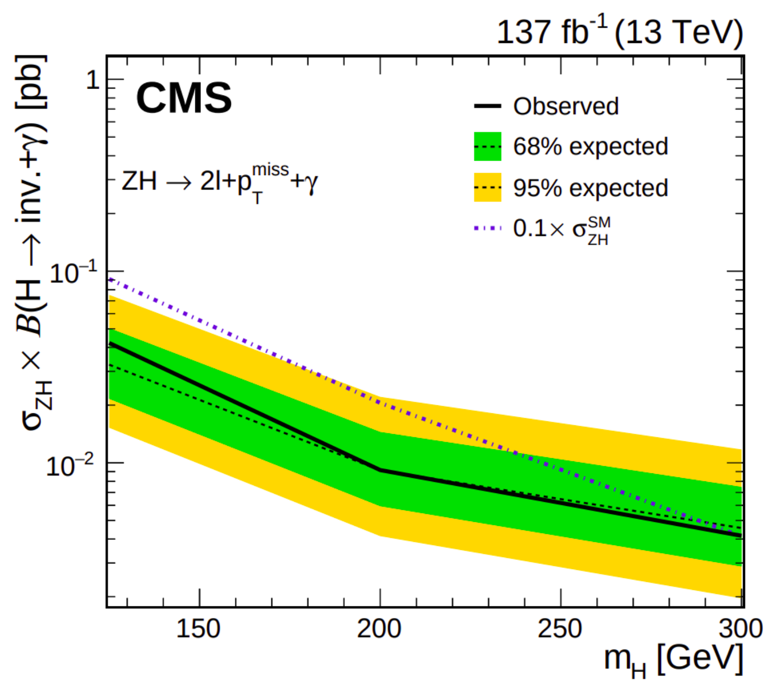

Dark photon experimental status

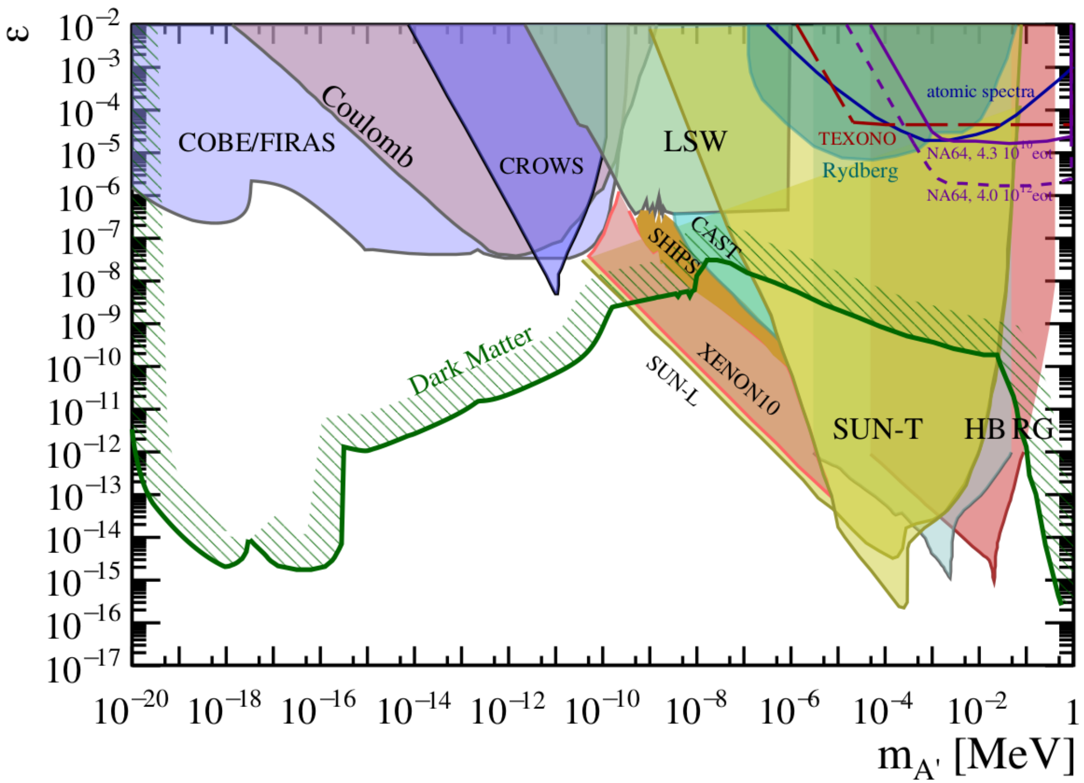

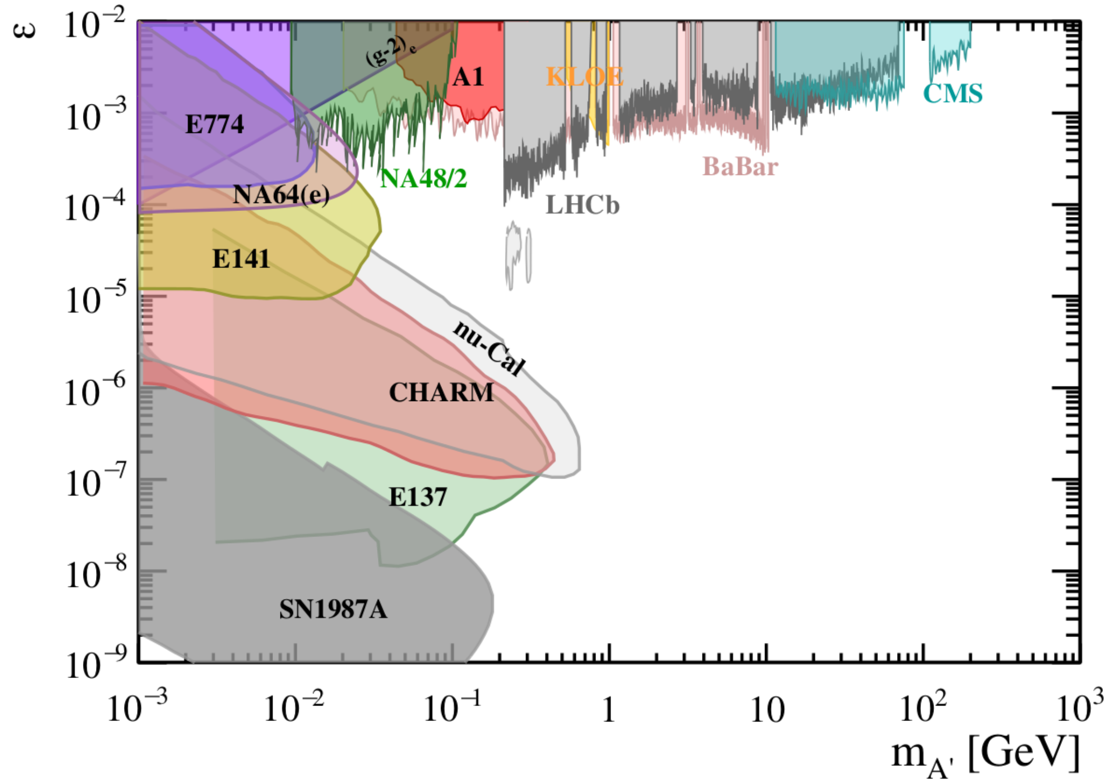

Dark photon experimental status